





















## The Ly $\alpha$ and Continuum Origins Survey. III. Investigating the link between galaxy morphology, merger properties and LyC escape

ALEXANDRA LE RESTE <sup>1</sup>, ANNE E. JASKOT,<sup>2</sup> JORDANNE BRAZIE,<sup>2</sup> CLAUDIA SCARLATA <sup>1</sup>, SOPHIA R. FLURY <sup>3</sup>,  
KAMESWARA B. MANTHA <sup>1</sup>, ALAINA HENRY,<sup>4,5</sup> MATTHEW J. HAYES <sup>6</sup>, GÖRAN ÖSTLIN <sup>6</sup>,  
ALBERTO SALDANA-LOPEZ <sup>6</sup>, TRINH X. THUAN <sup>7</sup>, MAXIME TREBITSCH <sup>8</sup>, XINFENG XU <sup>9,10</sup>,  
RICARDO O. AMORÍN <sup>11</sup>, FLORIANE LECLERCQ <sup>12</sup>, DANIEL SCHAEERER <sup>13,14</sup>, AARON SMITH <sup>15</sup>, CODY A. CARR <sup>16,17</sup>,  
JENS MELINDER <sup>6</sup>, M. S. OEY <sup>18</sup>, SWARA RAVINDRANATH <sup>19,20</sup>, MICHAEL RUTKOWSKI <sup>21</sup> AND BINGJIE WANG <sup>22,\*</sup>

<sup>1</sup>Minnesota Institute for Astrophysics, University of Minnesota, 116 Church Street SE, Minneapolis, MN 55455, USA

<sup>2</sup>Department of Astronomy, Williams College, Williamstown, MA 01267, USA

<sup>3</sup>Institute for Astronomy, University of Edinburgh, Royal Observatory, Edinburgh, EH9 3HJ, UK

<sup>4</sup>Center for Astrophysical Sciences, Department of Physics & Astronomy, Johns Hopkins University, Baltimore, MD 21218, USA

<sup>5</sup>Space Telescope Science Institute, 3700 San Martin Drive, Baltimore, MD 21218, USA

<sup>6</sup>Department of Astronomy, Oskar Klein Centre, Stockholm University, 106 91 Stockholm, Sweden

<sup>7</sup>Astronomy Department, University of Virginia, P.O. Box 400325, Charlottesville, VA 22904-4325, USA

<sup>8</sup>LUX, Observatoire de Paris, Université PSL, Sorbonne Université, CNRS, 75014 Paris, France

<sup>9</sup>Department of Physics and Astronomy, Northwestern University, 2145 Sheridan Road, Evanston, IL, 60208, USA.

<sup>10</sup>Center for Interdisciplinary Exploration and Research in Astrophysics (CIERA), 1800 Sherman Avenue, Evanston, IL, 60201, USA.

<sup>11</sup>Instituto de Astrofísica de Andalucía (CSIC), Apartado 3004, 18080 Granada, Spain

<sup>12</sup>CNRS, Centre de Recherche Astrophysique de Lyon UMR5574, Univ Lyon, Univ Lyon1, Ens de Lyon, F-69230 Saint-Genis-Laval, France

<sup>13</sup>Observatoire de Genève, Université de Genève, Chemin Pegasi 51, 1290 Versoix, Switzerland

<sup>14</sup>CNRS, IRAP, 14 Avenue E. Belin, 31400 Toulouse, France

<sup>15</sup>Department of Physics, The University of Texas at Dallas, Richardson, TX 75080, USA

<sup>16</sup>Center for Cosmology and Computational Astrophysics, Institute for Advanced Study in Physics  
Zhejiang University, Hangzhou 310058, China

<sup>17</sup>Institute of Astronomy, School of Physics, Zhejiang University, Hangzhou 310058, China

<sup>18</sup>University of Michigan, Department of Astronomy, 1085 S. University Ave, Ann Arbor, MI 48109, USA

<sup>19</sup>Astrophysics Science Division, NASA Goddard Space Flight Center, 8800 Greenbelt Road, Greenbelt, MD 20771, USA

<sup>20</sup>Center for Research and Exploration in Space Science and Technology II, Department of Physics, Catholic University of America, 620  
Michigan Ave N.E., Washington DC 20064, USA

<sup>21</sup>Minnesota State University-Mankato, Dept. of Physics and Astronomy, TN141, Mankato, MN 56001, USA

<sup>22</sup>Department of Astrophysical Sciences, Princeton University, Princeton, NJ 08544, USA

### ABSTRACT

Characterizing the mechanisms and galaxy properties conducive to the emission and escape of ionizing (LyC) emission is necessary to accurately model the Epoch of Reionization, and identify the sources that powered it. The Lyman-alpha and Continuum Origins Survey (LaCOS) is the first program to obtain uniform, multi-wavelength sub-kpc imaging for a sufficiently large sample (42) of galaxies observed in LyC to enable statistically robust studies between LyC and resolved galaxy properties. Here, we characterize the morphology and galaxy merger properties of LaCOS galaxies and investigate their connection with the escape fraction of LyC emission  $f_{esc}^{LyC}$ . We find strong anti-correlations between  $f_{esc}^{LyC}$  and radii ( $r_{20}$ ,  $r_{50}$ , and  $r_{80}$ ) measured in filters containing emission from star-forming regions, and with the asymmetry and clumpiness in F150LP, the bluest filter in our dataset, tracing UV continuum and Ly $\alpha$ . We find that  $\geq 48\%$  of LaCOS galaxies are visually classified as galaxy mergers. In LyC-emitters,  $\geq 41\%$  of the galaxies are galaxy mergers, LyC-emitting mergers have  $f_{esc}^{LyC}=0-16\%$ . Galaxies robustly identified as mergers in LaCOS are all at advanced stages of interaction, close to coalescence. The  $f_{esc}^{LyC}$  properties of mergers and non-mergers cannot be differentiated statistically, and we only find significant difference between the two populations in terms of their sizes, with mergers having larger sizes. We conclude that  $f_{esc}^{LyC}$  tends to be larger in galaxies with a small number of compact, centrally-located, UV-emitting star-forming regions, that merger represent a sizable fraction

of LyC-emitting samples at  $z \sim 0$ , and that mergers at advanced stages of interaction can facilitate the escape of LyC photons from galaxies.

## 1. INTRODUCTION

The escape fraction of ionizing radiation  $f_{esc}^{LyC}$  is a key parameter needed to model the Epoch of Reionization ( $z \gtrsim 5.5$ ), an important phase transition of the Universe when primordial astrophysical objects ionized the intergalactic medium (e.g. Robertson 2022). The escape fraction is defined as the ratio between the flux of hydrogen-ionizing (Lyman Continuum, LyC,  $\lambda < 912 \text{ \AA}$ ) photons that escape the interstellar and circumgalactic media of a given source, and that which is intrinsically produced by that source. Assumptions on the  $f_{esc}^{LyC}$  of high- $z$  sources can completely change the history of reionization (Finkelstein et al. 2019; Naidu et al. 2020; Lin et al. 2024): obtaining accurate constraints for this parameter is thus necessary to properly model the high- $z$  Universe. Due to the absorption of LyC photons by the remaining neutral fraction of the intergalactic medium, it is essentially impossible to detect LyC at  $z > 4$  (Inoue et al. 2014). In order to estimate the  $f_{esc}^{LyC}$  during the Epoch of Reionization, one must use indirect methods which include calibrations obtained at lower redshifts (see review in Jaskot 2025), Bayesian inference (Begley et al. 2022, 2024; Kreilgaard et al. 2024), or SED-fitting coupled with LyC escape prescriptions (Papovich et al. 2025; Giovino et al. 2025).

The two main astrophysical sources thought to participate in the reionization of the Universe are star-forming galaxies and Active Galactic Nuclei (AGNs). Star-forming galaxies emit LyC photons through their O and B stars, that efficiently produce LyC photons, and where strong stellar feedback helps clear the interstellar medium and facilitate LyC escape (Heckman et al. 2011; Trebitsch et al. 2017; Chisholm et al. 2017; Amorín et al. 2024; Flury et al. 2024; Carr et al. 2025; Komarova et al. 2025; Martin et al. 2024; Flury et al. 2025). AGNs produce LyC through heating onto their accretion disks, and are thought to have large  $f_{esc}^{LyC}$  ( $\sim 75\%$ ) (Cristiani et al. 2016; Grazian et al. 2018), although see e.g. Micheva et al. (2017); Smith et al. (2024). However, whether their number density and ionizing output at high- $z$  are sufficient to reionize the Universe is still under debate (Grazian et al. 2018; Hassan et al. 2018; Dayal et al. 2020; Matsuoka et al. 2023; Trebitsch et al. 2023; Harikane et al. 2023; Yeh et al. 2023; Madau et al. 2024; Grazian et al. 2024), making star-forming galaxies the candidates currently favored

by the community (Hassan et al. 2018; Dayal et al. 2020; Rosdahl et al. 2022; Trebitsch et al. 2022, 2023; Matsuoka et al. 2023; Yeh et al. 2023). Observations of LyC-emitting galaxies (LCEs) at intermediate and low redshift have brought substantial insights onto the properties of galaxies associated with LyC emission and escape. The role of both global (Leitet et al. 2013; Izotov et al. 2016, 2021, 2018, 2022; Flury et al. 2022a; Saldana-Lopez et al. 2022; Chisholm et al. 2022; Roy et al. 2024; Wang et al. 2019; Izotov et al. 2021; Xu et al. 2022; Vanzella et al. 2018; Mostardi et al. 2015; Steidel et al. 2018; Fletcher et al. 2019; Nakajima et al. 2020; Ji et al. 2020; Marques-Chaves et al. 2021; Pahl et al. 2021; Saxena et al. 2022) and sub-kpc scales (Kim et al. 2023; Marques-Chaves et al. 2024; Komarova et al. 2024; Le Reste et al. 2025a; Saldana-Lopez et al. 2025; Ji et al. 2025) galaxy properties into  $f_{esc}^{LyC}$  have been investigated, allowing for calibrations between galaxy properties and  $f_{esc}^{LyC}$  to be derived (Izotov et al. 2018; Chisholm et al. 2018, 2022; Flury et al. 2022a; Xu et al. 2022; Choustikov et al. 2024; Jaskot et al. 2024; Mascia et al. 2024; Leclercq et al. 2024; Saldana-Lopez et al. 2025). It is generally understood that LyC-emitting galaxies tend to have large specific star formation rates, high ionization states, produce stars in compact regions, and have low HI coverage on the line of sight to their LyC production sites (Jaskot 2025). Several mechanisms conducive to LyC escape from galaxies have been put forward in the literature, including suppressed feedback (Jaskot et al. 2017), ionizing feedback (Gazagnes et al. 2018, 2020; Flury et al. 2022a, 2025; Bait et al. 2024), stellar and supernova feedback (Chisholm et al. 2017; Amorín et al. 2024; Komarova et al. 2021, 2024; Flury et al. 2025) and bursty star formation (Trebitsch et al. 2017; Flury et al. 2025). However, what triggers the formidable star-forming episodes in the extreme galaxies leaking LyC photons is still not well understood.

Galaxy mergers have been suggested by several studies as a mechanism that could facilitate LyC escape from galaxies through their impact on star formation and gas morphology (Bridge et al. 2010; Bergvall et al. 2013; Purkayastha et al. 2022; Le Reste et al. 2024; Yuan et al. 2024; Zhu et al. 2024; Maulick et al. 2024). During gas-rich interactions, mergers repeatedly trigger starburst episodes following pericentric passages (Faria et al. 2025). Mergers tend to have significantly larger star-formation rates than isolated galaxies with otherwise similar properties, especially at later stages of interaction (Patton et al. 2013; Stierwalt et al. 2015; Fer-

\* NHFP Hubble Fellow

reira et al. 2025). By creating numerous massive stars, starbursts naturally increase the intrinsic production of LyC photons, as well as boost their escape through stellar and supernova-driven feedback (Trebitsch et al. 2017; Barrow et al. 2020; Ma et al. 2020; Choustikov et al. 2024). Additionally, tidal forces in mergers drive part of the gas away from the center of galaxies (Pearson et al. 2016), thus enhancing  $f_{esc}^{LyC}$  in lines-of-sights oriented away from tidal tails (Le Reste et al. 2024; Ejdetjärn et al. 2025). However, while galaxy interactions could theoretically help increase LyC production and escape, the existence and extent of this increase is not well characterized. In particular, there are currently very few constraints on the merger fraction and characteristic timescales in samples of confirmed LyC-emitters.

Simulations of  $z = 5 - 10$  galaxies using simple prescriptions for  $f_{esc}^{LyC}$  have shown promising results, indicating galaxy mergers could indeed enhance LyC escape (Kostyuk & Ciardi 2024). Yet, observational studies on the role of galaxy mergers in LyC-emitters ( $z \lesssim 3$ ) have so far remained limited to small samples (Le Reste et al. 2024; Maulick et al. 2024), or to samples where the identification of mergers, and sometimes, LyC-emitters, is challenging due to the high redshift ( $z \geq 3$ ) of sources (Zhu et al. 2024; Mascia et al. 2025). Finally, a few studies have reported LyC emission offset from centers of galaxies, and have proposed merger interactions as a possible explanation (Yuan et al. 2024; Gupta et al. 2024). However, the lack of continuum emission redward of the Lyman limit in the regions where the offset emission is detected warrants careful consideration, as it raises questions about the nature and origin of the observed LyC signal.

The most commonly employed methods for merger identification are close-pair detection and morphological analysis. However, several factors conspire to make the accuracy of those methods poor as redshift increases. In particular, for morphological characterization, the low-surface brightness features enabling the detection of advanced mergers fade rapidly with redshift ( $\propto (1+z)^4$ ), and galaxies become clumpier as a function of redshift (Guo et al. 2015), resulting in increased confusion between mergers and star-forming galaxies at  $z > 2$  (Abruzzo et al. 2018). For close pair analysis, lower mass companions may not be detected at high redshift, so that merger identification fails to detect robustly all but the highest mass, highest luminosity mergers. Therefore, studies in the  $z < 2$  Universe, where merger identification is the most accurate and the direct observation of LyC is possible, are needed to help constrain the role of mergers onto LyC emission and escape.

The Lyman alpha and Continuum Origins Survey (LaCOS) is a program that imaged 42 nearby ( $z \sim 0.3$ ) star-forming galaxies observed in LyC with the Hubble Space Telescope (Le Reste et al. 2025a). The goal of this survey is to identify the resolved galaxy properties linked to LyC emission and escape. Le Reste et al. (2025a) showed that  $f_{esc}^{LyC}$  correlates best with properties evaluated in the small apertures centered on the brightest UV clumps. This suggests that a small number of bright, unobscured UV-emitting clusters are responsible for the bulk of ionizing photons escaping on our line-of-sight. Saldana-Lopez et al. (2025) also found that LyC-emitters tend to have compact Ly $\alpha$  haloes which indicate a higher fraction of Ly $\alpha$  photons escaping directly from HII regions in strong LyC-emitters. Owing to the availability of relatively deep, high-resolution imaging across several bands and the sufficiently low redshift of the sample, LaCOS is uniquely suited to in-depth morphological studies and merger identification of LyC-emitting galaxies. In this paper, we derive parameters characterizing the morphology of galaxies in rest-frame UV and optical bands, to estimate if the morphology of galaxies across wavelengths can be used to estimate  $f_{esc}^{LyC}$  and get insights on the processes responsible for LyC escape. Additionally, we visually identify mergers and characterize the advancement of interactions, to assess if galaxy mergers constitute a large fraction of LyC-emitting galaxies and get insights on the timescales where LyC escape occurs in mergers.

This paper is structured as follows. In section 2 we describe the data and methods used to derive morphological parameters and merger properties. In section 3, we present the morphometrics for our sample, place them in the context of the  $z \sim 0.3$  galaxy population, and evaluate trends with  $f_{esc}^{LyC}$ . In section 4 we show the results of the merger characterization and estimate the impact of merger interactions on LyC properties. Finally, we discuss the results in section 5 and present a summary and conclusion in section 6.

Throughout this work, we assume a standard flat  $\Lambda$ CDM cosmology with  $H_0 = 70 \text{ km s}^{-1} \text{ Mpc}^{-1}$  and  $\Omega_m = 0.3$ .

## 2. DATA AND METHODS

### 2.1. LaCOS HST photometry

LaCOS (Le Reste et al. 2025a; Saldana-Lopez et al. 2025) is a cycle 30 HST program that imaged 42 nearby ( $z \sim 0.3$ ) star-forming galaxies observed in LyC as part of the Low- $z$  Lyman Continuum Survey and its extension including archival observations (Flury et al. 2022b, LzLCS+). The LzLCS is a flagship survey that observed 67 low- $z$  galaxies in LyC and significantly in-

creased the number of known LyC-emitting objects as well as extended the galaxy property parameter space for these objects (Flury et al. 2022a). LaCOS builds upon LzLCS+ by delivering high-resolution imaging for a subset of galaxies representative of the full survey, aimed at investigating the link between resolved galaxy properties and LyC emission and escape. About half (22) of the galaxies observed in LaCOS are confirmed LyC-emitters with  $f_{esc}^{LyC}=0.01 - 0.49$ , while the rest are either not detected or have low-significance detections ( $< 2\sigma$ ) with  $f_{esc}^{LyC} < 0.02$ . The availability of non-detections is crucial, since those galaxies serve as a control sample with the exact same set of observations and selection criteria as the LyC-emitters. LaCOS observations consist of imaging in 5 filters, including two rest-frame UV filters (F150LP, F165LP) and three rest-frame optical filters (F438W, F547M, F850LP). With a  $\sim 0.1''$  PSF ( $< 400$  pc physical scale) and the rich multiwavelength dataset available, it is uniquely suited to morphological studies of LyC emitters. We refer the readers to Le Reste et al. (2025a) for a description of the LaCOS data reduction. Below, we describe the methods used to measure the morphology of the galaxies and identify galaxy mergers in the sample.

## 2.2. Morphometrics

Non-parametric morphological estimators, also sometimes called morphometrics, are parameters characterizing the distribution of light in galaxies, that do not require assumptions on the shape of their light profile. A large number of such parameters have been developed, among which the concentration  $C^1$  (Abraham et al. 1994, 1996; Bershadsky et al. 2000), the asymmetry  $A$  (Elmegreen et al. 1992; Abraham et al. 1996; Conselice et al. 2000; Conselice 2003), the clumpiness  $S$  (Conselice 2003), the Gini coefficient  $G$  (Abraham et al. 2003; Lotz et al. 2004), and the second-order moment of brightest 20% of light  $M_{20}$  (Lotz et al. 2004) are the most well-known, though not an exhaustive list (see also Freeman et al. 2013; Wen et al. 2014; Pawlik et al. 2016).

To explore possible correlations between  $f_{esc}^{LyC}$  and the morphology of galaxies, we derive several morphometrics for LaCOS galaxies in all filters available. Specifically, we derive  $A$ ,  $C$ ,  $S$ ,  $G$ ,  $M_{20}$ , the shape asymmetry  $A_s$ , and the radii containing 20%, 50% and 80% of the light,  $r_{20}$ ,  $r_{50}$  and  $r_{80}$  using the commonly used package **statmorph** (Rodriguez-Gomez et al. 2019). We note that radii were already derived for LaCOS galaxies UV filters in Saldana-Lopez et al. (2025), but

using a different method based on integration in circular radii. Prior to deriving the morphological parameters, the images are background-subtracted using sigma-clipped median filtering and a 2D background model with the **Background2D** functions in **photutils**. Segmentation maps are generated with the **photutils detect\_sources** routine, using a  $1\sigma$  threshold to detect sources with a minimum of 8 pixels. The apparent boundaries of the galaxies are consistently identified in F547M filter images; for consistency, this filter was used to define the segmentation map for each galaxy. We note that the exact choice of the filter used to define segmentation maps has little impact on the morphometrics in **statmorph**, as the user-defined segmentation map is used to calculate noise properties. Different segmentation maps adapted to the calculation of specific parameters are derived by **statmorph**. Morphometrics are calculated for all galaxies and all filters available in LaCOS using the **SourceMorphology** class from **statmorph** and using the segmentation map defined using the F547M filter. We do not measure morphometrics in continuum-subtracted Ly $\alpha$  images produced from the combination of F150LP and F165LP and presented in Le Reste et al. (2025a). The patchiness of these continuum-subtracted maps prevents accurate segmentation, and due to the presence of Ly $\alpha$  absorption in several galaxies, morphometrics cannot be robustly derived using **statmorph**. Custom morphological parameters characterizing Ly $\alpha$  emission were derived and compared to  $f_{esc}^{LyC}$  in Saldana-Lopez et al. (2025), we refer the reader to this study for a comparison of Ly $\alpha$  morphology and LyC emission.

## 2.3. Merger identification

The first step to estimating the impact of mergers on LyC emission is to identify merging galaxies as accurately as possible in LaCOS. Galaxy merger identification typically either proceeds via close-pair searches, or morphological identification. The first method identifies galaxies in close proximity that have a high chance of merging in the future, searching for objects with small projected separations and relative velocity separations (Patton et al. 2000; Ventou et al. 2019). Morphological classification instead targets galaxies at relatively advanced stages of interaction, taking advantage of the fact that tidal gravitational forces significantly perturb the stars and interstellar medium of the galaxies involved in a merger (Holmberg 1941; Toomre & Toomre 1972; Conselice et al. 2000; Lotz et al. 2004). The identification of galaxy mergers through their morphology can be done either visually (Le Fèvre et al. 2000; Darg et al. 2010; Kartaltepe et al. 2015), using non-parametric morphological parameters (Conselice 2003; Lotz et al.

<sup>1</sup> Initially proposed as a visually-defined parameter (Morgan 1958; Kent 1985).



2004; Scarlata et al. 2007; Holwerda et al. 2011; Wen et al. 2014; Pawlik et al. 2016), or using machine learning (Ferreira et al. 2020; Walmsley et al. 2020; Pearson et al. 2019a). The later two methods require calibration, which can be done by using visual identification as a standard (Conselice 2003; Lotz et al. 2004, 2008; Walmsley et al. 2020), or with mock images from simulations, where the merger history is known (Pearson et al. 2019a; Ferreira et al. 2025).

All of these methods have drawbacks and advantages, so that the choice of an identification scheme strongly depends on the data on which it is performed. Close pair searches require both objects in the pair to have accurate redshifts, and is therefore typically limited to brighter objects in large-scale surveys. Additionally, this method does not allow for the identification of mergers at advanced stages, when the galaxies in a pair are too close to be resolved, or have already merged. Visual identification, while being the oldest of all methods, is still often employed as the human eye is uniquely suited to identifying subtle morphological patterns in the light profile of galaxies, and is the simplest method to implement for small sample sizes. However, it can be relatively biased, requiring a sufficiently large number of classifiers to yield accurate results, and requires crowdsourcing in the case of large samples (Lintott et al. 2008; Darg et al. 2010). Morphometrics, on the other hand are extremely convenient when exploring large datasets, as non-parametric morphological parameters can be derived in bulk. However, the validity of the criteria used to select mergers via morphometrics are 1) strongly dependent on the surveys they are derived from (such as the redshift and mass considered, see e.g. Abruzzo et al. (2018)), and 2) are typically calibrated using visual identification and thus, ultimately suffer from the same issues as visual identification. In particular, survey-to-survey signal-to-noise and wavelength coverage variations can strongly impact the validity of certain criteria (Lotz et al. 2008; Mager et al. 2018). Finally, machine learning (ML)-based approaches offer a new avenue for identifying mergers beyond non-parametric morphological estimators, by learning complex patterns in high-dimensional parameter spaces. In recent years, the training of ML algorithms has been performed on mock observations from simulations, alleviating the bias that could potentially be introduced by visual classification (Pearson et al. 2019a; Ferreira et al. 2025). However, similarly to morphometrics, the specificity of the training set and image quality can impact the adaptability and applicability of the models to real data (Domínguez Sánchez et al. 2023; Bickley et al. 2024).

LaCOS contains only 42 galaxies at  $z = 0.22 - 0.32$ , with specific galaxy property and imaging parameter spaces (Le Reste et al. 2025a). These make both morphometrics criteria developed for general galaxy surveys and the use of CNNs trained on mock images derived from simulations inadequate. While all of the galaxies have SDSS spectroscopy, they tend to have low stellar masses (with median  $M_* = 10^9 M_\odot$ , and as low as  $1.8 \times 10^8 M_\odot$ ), meaning that possible lower-mass companions may not have available spectroscopic data. Additionally, we expect mergers at later stages of interaction to be important for LyC emission, as this is when the largest enhancements in SFRs are found (Ferreira et al. 2025), and simulations looking at the post-merger  $f_{esc}^{LyC}$  evolution find the largest  $f_{esc}^{LyC}$  at coalescence (Kostyuk & Ciardi 2024). Thus, we choose to proceed with visual identification for our sample of 42 galaxies. To mitigate bias that could be introduced by visual identification, all members of the LaCOS collaboration were asked to perform the classification. In total, each galaxy was classified by 24 people.

Visual classification participants were shown image panels showing optical color-composite RGB (with B=F438W, G=F547M and R=F850LP), and single filter images of all galaxies, with both large-scale (24" on the side, corresponding to  $\sim 100$  kpc) and 20 kpc cutout images for color-composites, as shown in Figure 9 in Appendix A. Importantly, the color-composites are made by normalizing the flux in each filter to its own maximum, to highlight structural features across all bands. LaCOS galaxies are highly star-forming, thus traditional RGB images using optical filters scaled to a common maximum are fully dominated by emission in the bluer bands, eclipsing faint isophotes from redder bands. In many cases, the morphological features that allow for the classification of LaCOS objects as mergers are mostly visible in the redder optical band.

In addition to classifying the galaxies in merger and non-merger categories, the classifiers were asked to visually assess the merger stage to obtain a measure of the advancement of the merger. To do so, we used broad categories split between pre-interaction and post-coalescence (following Mantha et al., in prep. and similar to the approaches in e.g. Veilleux et al. (2002) and Pan et al. (2019)). Each merger categories has a score  $s_i$  ranging from 1 to 4 tracking the advancement of the merger. The specific options classifiers could choose, and associated merger stage scores were:

1. **Not a merger:** no score.
2. **Pre-interaction:**  $s_i = 1$ . Well-separated galaxies that do not show any morphological distortion,

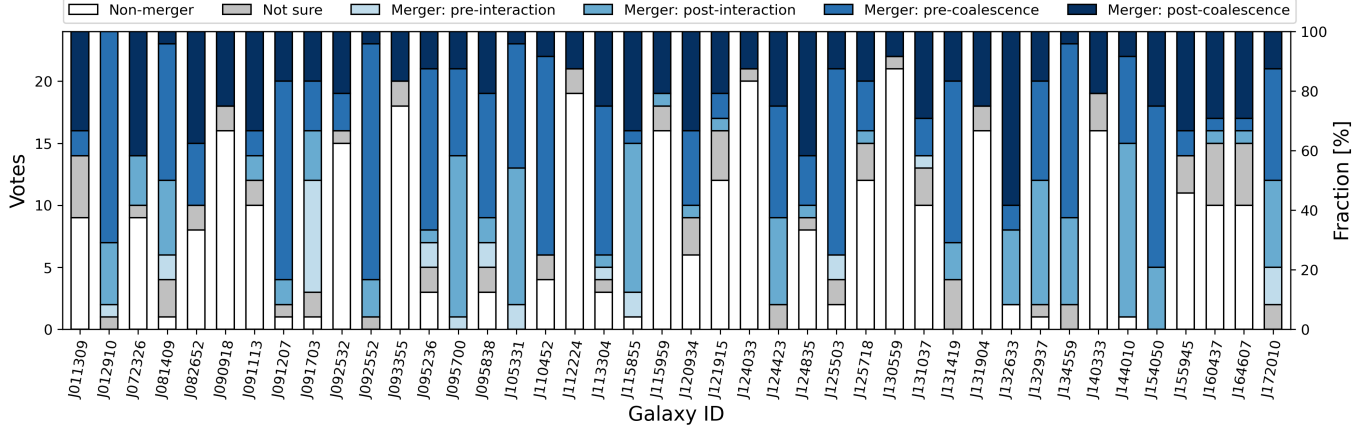


**Figure 1.** Distribution of visual merger classification votes for LaCOS galaxies. Each galaxy was classified by 24 of the LaCOS collaboration members. There is a large degree of variation in the answers of individual classifiers, illustrating the importance of a large number of classifiers to obtain a consensus answer.

- i.e., incoming pairs, before the first pericenter passage.
3. **Post-interaction:**  $s_i = 2$ . Well-separated galaxies, but showing morphological distortion.
  4. **Pre-coalescence:**  $s_i = 3$ . Two (or more) galaxies embedded within each-other's light envelopes and displaying disturbed morphological features.
  5. **Post-coalescence:**  $s_i = 4$ . The galaxies' central core regions have merged into one or are visibly indistinguishable, but the system has disturbed morphological features (e.g. tidal tails, faint asymmetric components, shells).
  6. **Not sure:** no score.

We note that although the classification scheme outlined above divides galaxy mergers into distinct visual categories based on morphological features, there is overlap and potential ambiguity between these categories, which do not exactly map onto specific merger timescales. Nevertheless, these classifications still provide a useful measure of the overall progression of a merger.

Figure 1 displays the distribution of votes resulting from the visual classification, demonstrating significant dispersion in classification outcomes. For this reason, and to select solely for mergers and limit the inclusion of non-merging irregular galaxies that could potentially be present in the sample, we establish a strict criterion for identifying a galaxy as a merger. We take into account all of the votes towards any merger category (with scores  $s_i = 1 - 4$ ) and establish a threshold based on the fraction of votes going to any merger category  $P_{\text{merg}} = \frac{N_{\text{merg}}}{N_{\text{tot}}}$ . For each galaxy, the merger identification process through voting can be approximated by a

series of Bernoulli trials with yes/no answers. To set a baseline for classification, we therefore consider a binomial distribution, with random classification yielding a 50% chance that a galaxy is classified as a merger for each vote. We use the `histogram` package developed in (Flury et al. 2022b) to calculate the  $3\sigma$  confidence interval for a binomial distribution with 24 choose 12 assuming maximal variance in each vote. This corresponds to a merger vote fraction  $P_{\text{merg}} = 79\%$ . We therefore select all galaxies with  $P_{\text{merg}} \geq 79\%$  as robust galaxy mergers. In Appendix B we compare the visual classification to traditional classifications using morphometrics (Conselice 2003; Lotz et al. 2008; Pawlik et al. 2016). To obtain a broad measure of the advancement of a merger, we calculate the merger stage as  $s_{\text{merg}} = \frac{\sum_i s_i}{N_{\text{merg}}}$ , the average of scores for votes towards merger classifications.

### 3. MORPHOLOGY OF THE LACOS GALAXIES

#### 3.1. Correlation with the escape fraction

Here, we explore and characterize possible correlations between galaxy morphology and  $f_{\text{esc}}^{\text{LyC}}$  using morphometrics measured at different wavelengths in LaCOS filters. To that aim, we calculate the Kendall  $\tau$  rank correlation coefficient between  $f_{\text{esc}}^{\text{LyC}}$  and the various morphometrics derived in this work. The Kendall  $\tau$  coefficient measures the association between two variables, and thus provides an estimate of the strength of a correlation. To enable the proper treatment of upper limits, the Kendall  $\tau$  coefficients and associated  $p$ -values are calculated using an approach allowing for the inclusion of censored data (Isobe et al. 1986). We use the code adapted from Flury et al. (2022a) and presented in Herenz et al. (2025). Following the convention in other LaCOS manuscripts (Le Reste et al. 2025a; Saldana-Lopez et al. 2025), we deem a correlation ( $\tau > 0$ ) or

anti-correlation ( $\tau < 0$ ) robust when  $p < 1.35 \times 10^{-3}$  and tentative when  $1.35 \times 10^{-3} < p < 0.05$ . These respectively correspond to a  $> 3\sigma$  and  $2 - 3\sigma$  confidence that the null hypothesis, stating a coefficient of this magnitude or higher could have arisen purely by chance, can be rejected.

In Figure 2, we present a heatmap showing the Kendall  $\tau$  coefficient and associated  $p$ -values between morphometrics and  $f_{esc}^{LyC}$  in all available LaCOS HST filters. For robust correlations, the Kendall  $\tau$  value is shown in black bold fonts, for tentative correlations it is shown in gray bold font. Non-significant correlations are shown in normal gray fonts. There is, for most filters, a relatively high degree of anti-correlation ( $\tau < -0.33$ ,  $p < 8 \times 10^{-4}$ ) between  $f_{esc}^{LyC}$  and the size of the galaxies as measured using  $r_{20}$ ,  $r_{50}$  and  $r_{80}$ . The only exception is for filter F547M, that only shows a tentative anti-correlation between galaxy sizes and  $f_{esc}^{LyC}$ . This may be explained by the fact that the filters where an anti-correlation can be found tend to trace star-forming regions. Indeed, F150LP and F165LP are both rest-frame UV filters, and F438W traces emission at rest-frame blue optical wavelengths, therefore containing emission from recently formed massive stars. F850LP, while sampling rest-frame red optical wavelengths, does include H $\alpha$  emission at the edge of the bandpass for 29 of the galaxies in LaCOS (with  $z \gtrsim 0.27$ ), also tracing recent star-formation. Isolating galaxies with H $\alpha$  contribution in the F850LP bandpass, we get a significantly stronger anti-correlation between  $r_{50}$  and  $f_{esc}^{LyC}$  ( $\tau = -0.43$ ,  $p = 4.5 \times 10^{-4}$ ). Accordingly, for galaxies without H $\alpha$  in the F850LP bandpass, we do not find a statistically significant anti-correlation between  $f_{esc}^{LyC}$  and  $r_{50}$  ( $\tau = -0.21$ ,  $p = 0.26$ ). This would indicate that galaxies with small sizes and specifically, small star-forming regions, tend to have elevated escape fractions. A link between small UV-emitting regions and  $f_{esc}^{LyC}$  has been shown by several previous studies (Kim et al. 2023; Flury et al. 2022a; Le Reste et al. 2025a). Here we show that this may also be found in optical filters covering emission associated with recent star-formation.

Another strong anti-correlation is seen between the asymmetry in the F150LP filter and  $f_{esc}^{LyC}$ . The F165LP filter also shows a tentative anti-correlation between asymmetry and  $f_{esc}^{LyC}$ . Asymmetry in the rest-frame optical has been used as a tracer of galaxy interaction (e.g. Conselice et al. 2000; Conselice 2003), but here we find no association between asymmetry measured in the optical and  $f_{esc}^{LyC}$ . UV emission solely traces recent star-forming regions, while the redder stellar continuum traces older stars. As such, the asymmetry parameter in the UV can be seen as a proxy for the spatial dis-

tribution and number of star-forming clumps. Therefore, the anti-correlation between the F150LP asymmetry and  $f_{esc}^{LyC}$  likely indicates that galaxies with a small number of centrally-located UV clumps are more likely to have large  $f_{esc}^{LyC}$ . This is also reflected in the anti-correlation between  $f_{esc}^{LyC}$  and the clumpiness in F150LP, which measures the fraction of light in small scale structures, and  $f_{esc}^{LyC}$ . The stronger anti-correlations found in F150LP as compared to F165LP could be due to the fact that F150LP contains Ly $\alpha$  emission, and that the sampled UV continuum is bluer, thus better tracing the regions emitting LyC.

Le Reste et al. (2025a) found a strong correlation between Ly $\alpha$  observables (specifically the luminosity and EW) measured in small apertures around the brightest UV emission region and  $f_{esc}^{LyC}$  on the line-of-sight. This was interpreted as the escaping LyC emission being contributed by a small number of bright, unobscured UV clumps. The anti-correlation between morphometrics in the F150LP filter, which contains Ly $\alpha$  emission and stellar UV continuum, also supports this hypothesis. This is additionally supported by results in Saldana-Lopez et al. (2025), which measured the Ly $\alpha$  halo properties of LaCOS galaxies. They found a strong anti-correlation between  $f_{esc}^{LyC}$ ,  $r_{20}$  and  $r_{50}$  as measured in the Ly $\alpha$  images ( $\tau < -0.41$ ,  $p < 10^{-4}$ ). This is also in line with their results on the Ly $\alpha$  halo fraction, which showed that the Ly $\alpha$  cores, instead of the haloes, drive the correlation with  $f_{esc}^{LyC}$ . We note that Saldana-Lopez et al. (2025) found a strong correlation between  $f_{esc}^{LyC}$  and  $r_{90}/r_{20}$  in Ly $\alpha$ , a measurement analogous to the concentration parameter as defined in `statmorph`. Here, we do not find any correlation between the concentration parameter in F150LP and  $f_{esc}^{LyC}$ , which may be due to the filter containing both Ly $\alpha$  and UV continuum emission.

We fit log-log and log-linear relations between  $\log_{10} f_{esc}^{LyC}$  and the morphometric parameters found to significantly anti-correlate with  $f_{esc}^{LyC}$  shown on Figure 3. For that purpose, we use the python package `linmix` (Kelly 2007), that performs linear fits to censored datasets using a Bayesian framework. This allows for the accurate treatment of upper limits in the fits to  $\log_{10} f_{esc}^{LyC}$ . Specifically, for each parameter  $x$ , we fit a function of the form:

$$\log_{10} f_{esc}^{LyC} = a + b \cdot x$$

with fitting parameters  $a$  and  $b$  shown in Table 1. Either the log-log or log-linear fit is presented, depending on which yields the lower  $\chi^2$  value. As with previous correlations involving single variables and  $f_{esc}^{LyC}$ , we find a scatter of  $\sim 0.3$  dex around the fit.

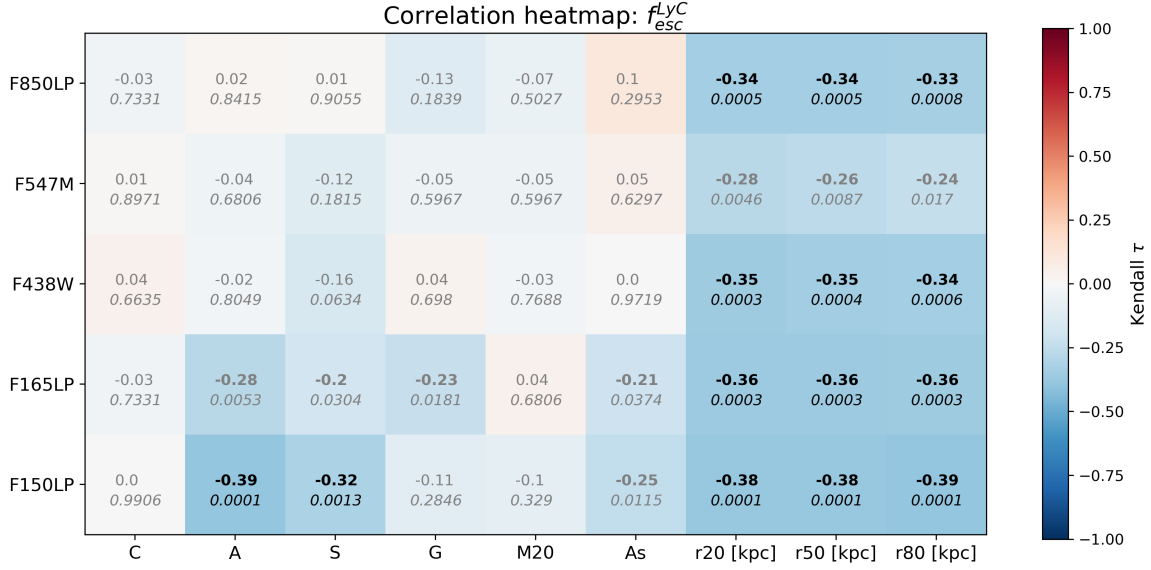


**Figure 2.** Heatmap showing the Kendall  $\tau$  correlation coefficient and associated p-value between non-parametric morphological estimators and the  $f_{esc}^{LyC}$  for LaCOS galaxies in different filters. The Kendall  $\tau$  values are shown, with corresponding p-values displayed directly below in italic. Robust correlations ( $p < 1.35 \times 10^{-3}$ ) are indicated in bold black text, tentative correlations ( $0.05 < p \leq 1.35 \times 10^{-3}$ ) in bold gray text and non-significant correlations ( $p \geq 0.05$ ) in regular gray text.

**Table 1.** Fitting parameters and scatter around the fit for the log-log and log-linear relations between  $\log_{10} f_{esc}^{LyC}$  and morphometrics  $x$ . The radii are in kpc.

$x$	a	b	$\sigma$
$\log_{10} r_{50, F150LP}$	$-1.98 \pm 0.08$	$-1.9 \pm 0.31$	0.27
$\log_{10} r_{50, F165LP}$	$-2.19 \pm 0.1$	$-1.43 \pm 0.27$	0.28
$\log_{10} r_{50, F438W}$	$-2.18 \pm 0.11$	$-1.45 \pm 0.29$	0.29
$\log_{10} r_{50, F850LP}$	$-1.91 \pm 0.09$	$-1.41 \pm 0.3$	0.31
$\log_{10} A_{F150LP}$	$-3.02 \pm 0.22$	$-2.45 \pm 0.43$	0.31
$S_{F150LP}$	$-1.28 \pm 0.15$	$-5.63 \pm 1.2$	0.32

### 3.2. Comparison to the general galaxy populations

We have explored correlations between  $f_{esc}^{LyC}$  and morphometrics in different filters in the previous section. In the following, we compare the morphometrics derived in LaCOS to those of the general galaxy population to get a sense of the parameter space occupied by LyC emitters and candidates.

We compare LaCOS morphometrics to those available for galaxies in the Cosmic Evolution Survey (Scoville et al. 2007, COSMOS). The COSMOS survey is very well suited to such a comparison, as it is a wide, multi-wavelength survey of galaxies covering a large redshift range and having HST imaging. We note, however, that at the redshift range of interest, COSMOS galaxies do not have LyC observations. Therefore, we do not know if, or which of the COSMOS galaxies are LyC-emitters. Nevertheless LyC-emitters are rare at  $z \sim 0$ , so we ex-

pect a very small number of LyC-emitters in COSMOS in the redshift range considered, if any.

To enable comparisons between LaCOS and COSMOS, we select COSMOS galaxies at the same redshifts as LaCOS objects ( $z = 0.22 - 0.32$ ) using the spectroscopic redshift information in Khostovan et al. (2025), yielding an initial sample of 3573 galaxies. While morphometrics have been derived for COSMOS in Scarlata et al. (2007), differences in methods in statmorph and the dedicated software developed for the purpose of analyzing COSMOS galaxies could cause systematic differences in morphometrics and bias the comparison. Therefore, we adopt an approach similar to that employed in Scarlata et al. (2007), but using statmorph to compare COSMOS and LaCOS morphometrics. First, we use the Python SExtractor implementation sep (Bertin & Arnouts 1996; Barbary 2016) to derive segmentation maps and replace the pixels from sources in the field other than the main target with noise to create clean images. We then use the semiminor and semi-major axes  $a$  and  $b$  retrieved by sep to calculate the ellipticity  $e = 1 - b/a$  and position angle for the source. Additionally, we use the source flux to define a "total radius"  $R_{tot}$  through integration in circular apertures and extract stamps around the targets that are  $3 \times R_{tot}$  in size. We use the package petrofit to calculate the Petrosian radius in the masked stamps. Finally, we derive an initial segmentation map that is an ellipse of major-axis equal to the Petrosian radius and with ellipticity and position angles as derived using sep. We then



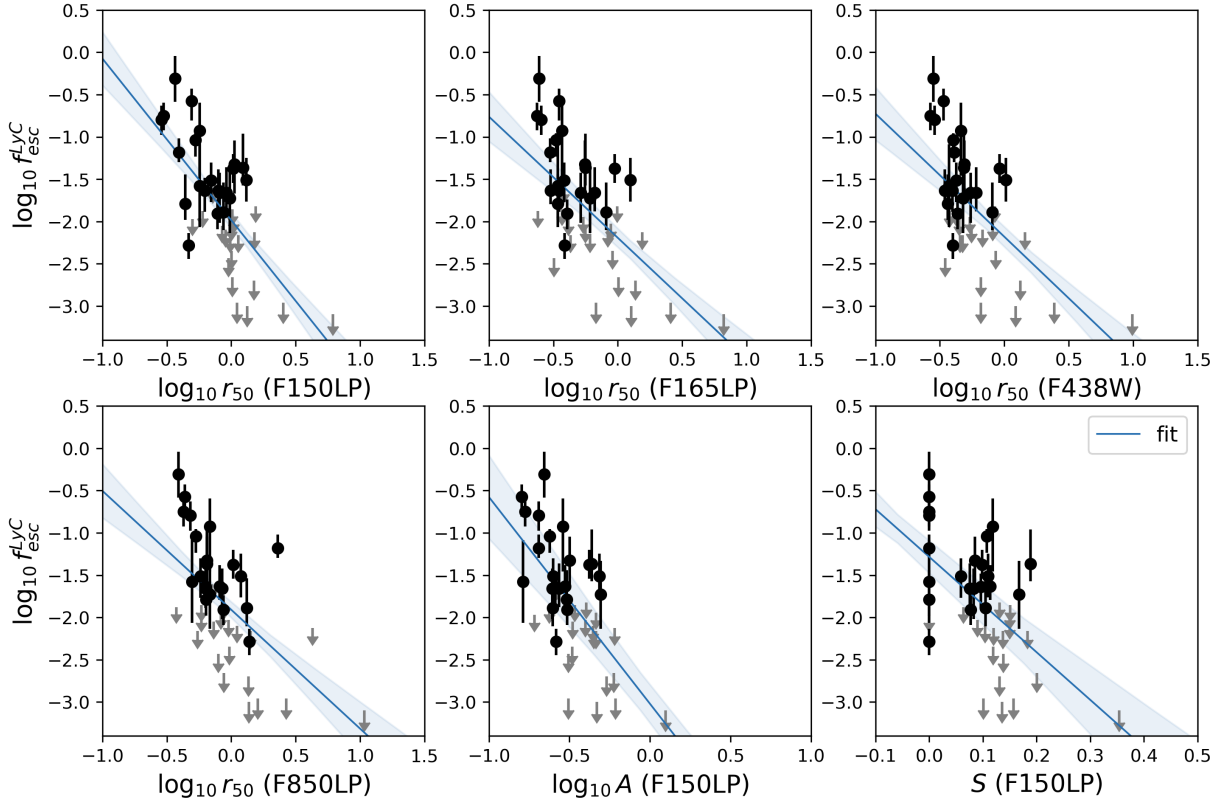


**Figure 3.** Fits between  $f_{esc}^{LyC}$  and the morphometrics found to be robustly anti-correlated with  $f_{esc}^{LyC}$ .

feed the corresponding stamps and segmentation maps to statmorph for the calculation of morphometrics. For COSMOS galaxies, we use the HST/ACS F814W mosaic images, with 0.03'' pixel scale, retrieved through the NASA/IPAC Infrared Science Archive. Cutouts could not be retrieved for 156 of the COSMOS galaxies with matching redshift as they were outside of the HST/ACS mosaic coverage. Additionally, morphometrics calculation failed for 400 galaxies due to contamination by neighboring stars and sources, incomplete HST coverage, or imaging artifacts. This results in 3017 COSMOS galaxies with redshifts matched to LaCOS and valid morphometrics. We re-derive LaCOS morphometrics in the F850LP filter (close to F814W in terms of wavelength coverage) using the same method as that applied to COSMOS galaxies. We note that the morphometrics derived for the comparison to COSMOS images in LaCOS have values similar as when using the method described in 2.2. The comparison of the morphometrics between LaCOS and COSMOS galaxies is shown in Figure 4.

Generally, and in agreement with the correlation coefficients shown in Figure 2, the LyC-emitters and non-emitters in LaCOS tend to occupy similar parameters spaces in  $M_{20}$ , Gini,  $A$ ,  $A_s$ ,  $C$  and  $S$  when measured in the optical. We run K-S tests for all morphomet-

rics between the LaCOS and COSMOS samples, and find that the LaCOS galaxies have significantly larger Gini,  $A$  and  $A_s$  parameters and smaller  $r_{20}$ ,  $r_{50}$ , and  $r_{80}$  in the optical than the general galaxy population at  $z \sim 0.3$  (with  $p < 1.35 \times 10^{-3}$ ). This may be partly due to sample selection, as one of the criteria used to select LzLCS galaxies required large  $\Sigma SFR$ , necessarily yielding galaxies with small radii and large star formation rates. However, and in accordance with results from 3, LyC-emitters have the smallest sizes, as compared to both to non LyC-emitters in LaCOS and the general galaxy population. Apart from their radii, the LyC-emitters and non-emitters in LaCOS do share similar parameters space. We therefore conclude that when it comes to concentration, asymmetry, Gini and  $M_{20}$ , any difference in morphologies between LaCOS galaxies and COSMOS is likely due to the criteria used to select LyC candidates in LzLCS, and in particular requirement on  $\Sigma SFR$  as outlined above. Interestingly, LaCOS galaxies are located in the part of the  $M_{20}$ -Gini parameter space where galaxy mergers tend to be found (Lotz et al. 2008). In the following, we explore the galaxy merger properties of LyC-emitters and non-emitters in LaCOS.

#### 4. MERGER PROPERTIES OF LACOS GALAXIES

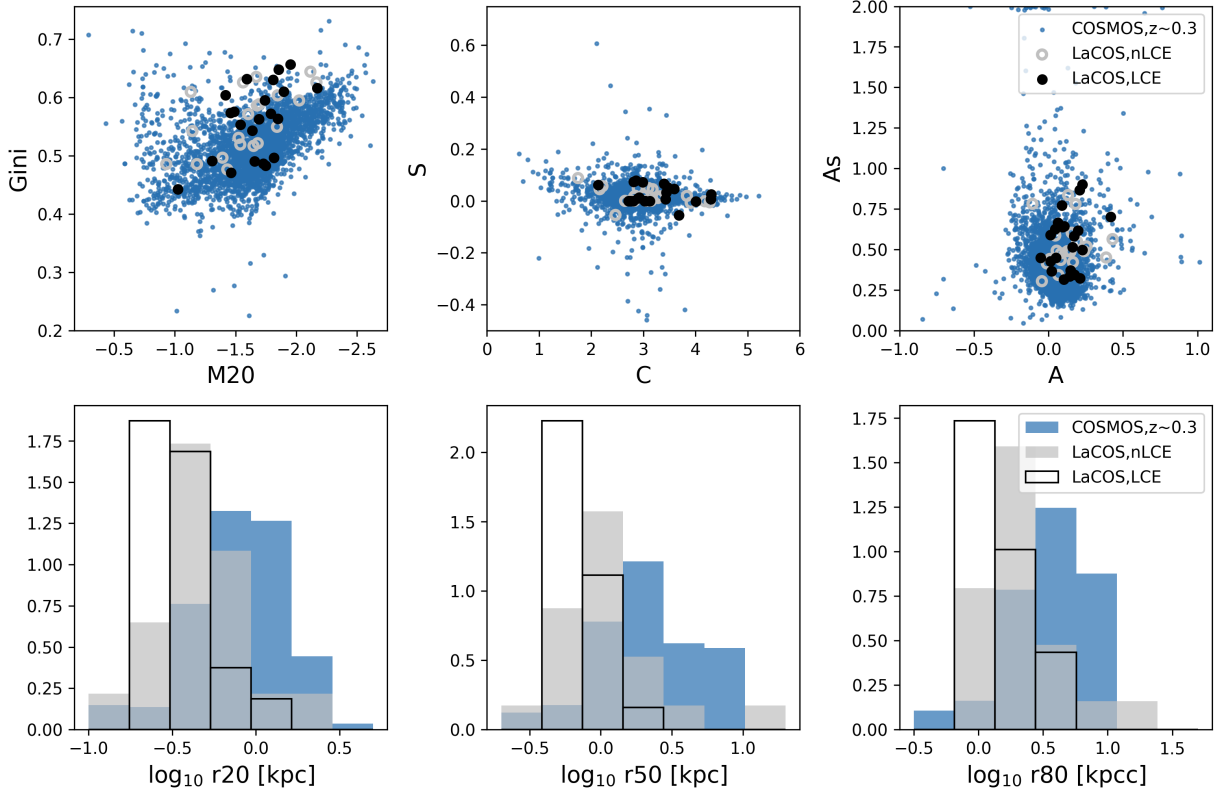


**Figure 4.** Comparison of the morphometrics parameter space for LaCOS galaxies as measured in the F850LP filter (black for LyC-emitters and gray for galaxies with upper limits) as compared to COSMOS galaxies at similar redshifts ( $z \sim 0.3$ ), with morphometrics measured in F814W (shown in blue). On the top panels, from left to right, we show the M20-Gini, C-S and A-A<sub>s</sub> diagrams. On the bottom panels, from left to right we show density plots for  $r_{20}$ ,  $r_{50}$  and  $r_{80}$ .

Here, we describe the results of the merger identification and stage evaluation as described in section 2.3. Specifically, we describe the merger fraction in LaCOS, for LyC emitters and non-emitters specifically, and the broad timescales of the merger interaction for galaxies identified as robust mergers. Figure 5 shows color-composite images of the galaxies identified as mergers and with low merger vote fraction on the same physical scale, with  $f_{esc}^{LyC}$  and merger information (merger vote fraction, merger stage) displayed next to each cutout.

#### 4.1. Merger fractions

Following visual identification, 48% of the LaCOS galaxies are identified as secure mergers ( $P_{merg} \geq 79\%$ , corresponding to  $3\sigma$ ), while the rest have low merger vote fraction ( $P_{merg} < 79\%$ ). When looking at LyC-emitters specifically, 41% of the LCEs are identified as secure mergers, while 55% of the nLCEs are identified as secure mergers. These values are to be compared with the merger fractions for galaxies in the local Universe ( $< 5\%$  Allam et al. 2004; Lotz et al. 2008; Conselice et al. 2009; Darg et al. 2010), for star-forming galaxies ( $\sim 10\%$  Lotz et al. 2008; Kaviraj et al. 2015; Duncan et al. 2019), and for highly star-forming galax-

ies or starbursts (20-50% Robaina et al. 2009; Pearson et al. 2019b). Both LyC emitters and non-emitters show a substantially larger merger fraction than local star-forming galaxies, similar to the fractions found in starburst galaxies. This is likely due to the criteria used to select LyC-emitters in LzCLS, based on either blue UV  $\beta$  slopes, large  $[O_{III}]/[O_{II}]$  line ratios tracing high ionization states, or large star formation rate surface densities  $\Sigma SFR$  (Flury et al. 2022b), leading to the selection of highly star-forming galaxies. Given mergers can efficiently trigger starbursts, thus could readily explain the high fraction of mergers found in both LyC and non-LyC-emitting galaxies in LaCOS.

#### 4.2. Visually identified merger stages

Next, we examine the broad timescales associated with the robust merger population identified in LaCOS, as measured by the merger stage introduced in 2.3. Among the 20 mergers in LaCOS, we identify 4 galaxies with morphologies consistent with post-interaction ( $1.5 \leq s_{merg} < 2.5$ ), and 16 galaxies near-coalescence ( $2.5 \leq s_{merg} < 3.5$ ). We do not find any pairs in pre-interaction stages or post-coalescence galaxies. Thus, all LaCOS galaxies securely identified as mergers are

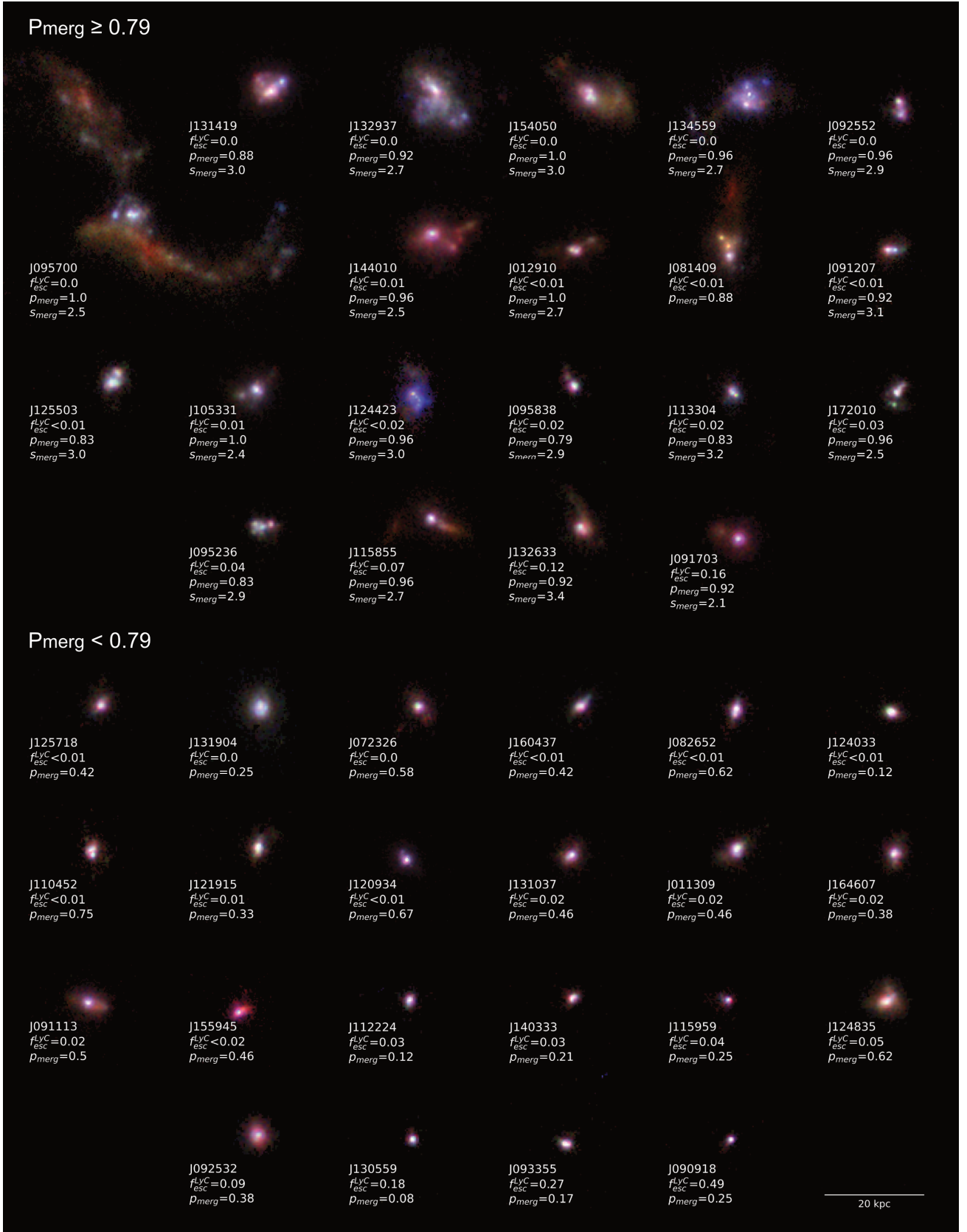


**Figure 5.** RGB images of LaCOS galaxies, split according to the fraction of merger votes. The top most panels show galaxies with  $P_{\text{merg}} \geq 79\%$ , robustly identified as mergers ( $\geq 3\sigma$ ), while the galaxies on the bottom panels show galaxies with low fraction of merger votes. Next to each galaxy, we show the values for  $f_{\text{esc}}^{\text{LyC}}$ , fraction of merger votes, and the merger stage. Galaxies are organized by increasing  $f_{\text{esc}}^{\text{LyC}}$  from top to bottom and left to right for the robust mergers and the galaxies with low merger vote fractions. A bar on the lower bottom right corner indicates the 20 kpc scale .

at advanced stages of interaction, having undergone at least one, or currently undergoing peri-center passages. We visually estimate the separation between nuclei in merging galaxies, and find a median projected separation of 1.4 kpc. Comparison to simulated galaxy mergers with similar projected distance in [Patton et al. \(2024\)](#) indicate a relatively short timescale to the merger at such projected distances, with the galaxies likely to merge within a few 100 Myr. In Figure 6 we show histograms of the merger stage for LCE and nLCEs respectively in the robust merger population. All the non-LyC leaking galaxies identified as mergers are in near-coalescence stages, while LCEs span a slightly larger interaction stage. Nevertheless, we cannot differentiate the samples through a KS test ( $p = 0.3$ ) so that the apparent difference is likely due to small number statistics. We do not find any correlation between  $f_{esc}^{LyC}$  and the merger stage, as shown in Figure 6 (with Kendall  $\tau = -0.089, p = 0.53$ ). This is likely due to the very narrow range in merger stages sampled by LaCOS, that yields too small of a dynamic range to accurately evaluate the impact of the merger stage on  $f_{esc}^{LyC}$ . However, the narrow merger stage distribution in LaCOS may indicate that LyC emission in mergers happen in a relatively narrow timescale in the interaction, at the very end of it. Alternatively, if starbursts are preferentially triggered at specific stages of a merger, then the selection process favoring starbursts is likely to yield galaxies at these particular points during the merger. Surveys investigating the ionizing properties of general galaxy merger samples will be required to draw definitive conclusions on the timescales and merger configurations conducive to LyC emission.

#### 4.3. Properties of robust and low-probability merger

Finally, we look at the properties of secure mergers and galaxies with low merger vote fraction. Figure 7 displays histograms of the merger and low merger vote fraction galaxies for various galaxy properties, including the stellar mass, star formation rate and star formation rate surface density, oxygen abundance, dust extinction, redshift,  $O_{32}$ , UV  $\beta$  slope, F165LP  $r_{50}$ ,  $f_{esc}^{Ly\alpha}$ ,  $f_{esc}^{LyC}$  and LyC luminosity. The values are obtained from [Flury et al. \(2022b\)](#) for most properties, and [Le Reste et al. \(2025a\)](#) for  $r_{50}$  and  $\Sigma SFR$  (with star formation rate measured using  $H\beta$  fluxes). We note the F165LP  $r_{50}$  values are different from those obtained with `statmorph` presented above as they employ different segmentation maps using integration in circular radii and a custom script. We run Kolmogorov-Smirnov (KS) tests using the `scipy` function `kstest` on all the properties, to assess whether or not the samples are statistically differ-

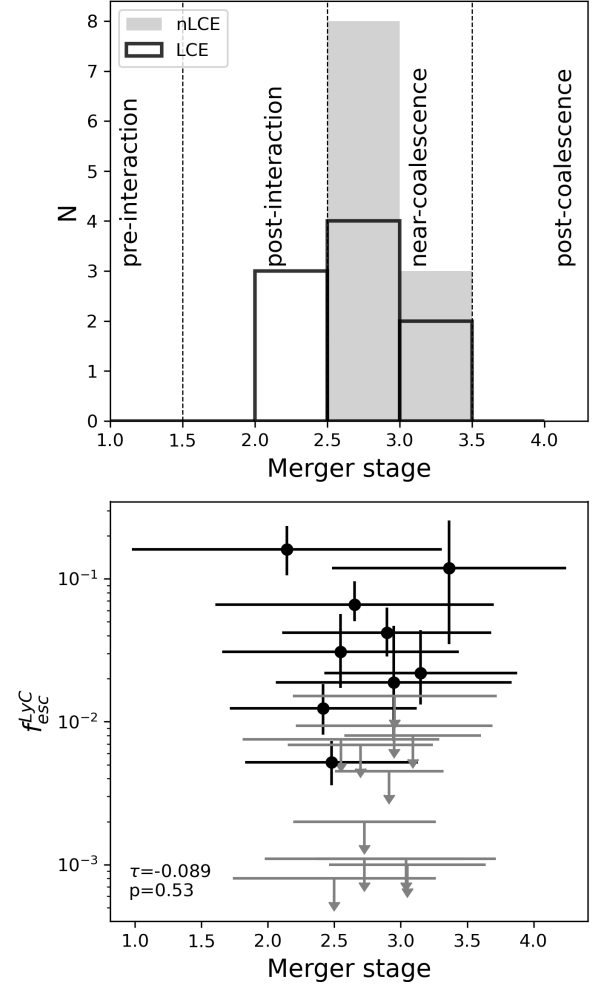


**Figure 6.** Merger stage and  $f_{esc}^{LyC}$ . Top: Histogram showing the merger stage for LyC-emitting (in black) and non LyC-emitting (in gray) galaxies with  $P_{merg} \geq 79\%$ . The galaxies identified as robust mergers in LaCOS all are at relatively advanced stages of interaction, with most being close to coalescence. Bottom:  $f_{esc}^{LyC}$  as a function of the merger stage for galaxies with  $P_{merg} \geq 79\%$ . The Kendall  $\tau$  and associated  $p$ -value characterizing the strength of the correlation are shown on the bottom left corner.

ent. We find that the samples differ in a statistically significant ( $p < 1.35e-3$ ) manner only in terms of their UV sizes  $r_{50}$ . Robust mergers and non-mergers differ tentatively ( $1.35e-3 < p < 0.05$ ) for  $\Sigma SFR$ , the  $O_{32}$  line ratio, the stellar mass, and metallicity as traced by the oxygen abundance. Specifically, robust galaxy mergers tend to have larger  $r_{50}$  (and hence, marginally lower  $\Sigma SFR$ ), marginally lower  $O_{32}$  line ratios, marginally larger stellar masses and marginally larger metallicities.

Examining the  $f_{esc}^{LyC}$  properties of robust galaxy mergers, they have escape fractions spanning the range  $f_{esc}^{LyC} = 0 - 16\%$ . Instead, the galaxies with low galaxy



merger vote fraction span  $f_{esc}^{LyC} = 0 - 49\%$ . The galaxies with low merger vote fractions contain the galaxies with the three highest  $f_{esc}^{LyC}$  of the LaCOS sample, explaining their larger average  $f_{esc}^{LyC}$ . However, we do not find evidence that their  $f_{esc}^{LyC}$  distribution differ significantly from that of the sample of galaxy mergers when running a K-S test ( $p = 0.09$ ), meaning the difference likely arises due to the rarity of strong LyC emitters and the small samples sizes. In the following, we discuss the differences between the merger and non-merger samples, and what they could indicate regarding the classification of LyC-emitters.

## 5. DISCUSSION

### 5.1. Are galaxy mergers accurately identified in LaCOS?

In section 4 we have shown that all the mergers identified visually with high confidence ( $P_{merg} \geq 79\%$ ) in LaCOS are at advanced stages of interaction, having undergone at least one peri-center passage or being close to merging. Additionally, the main difference between the robust mergers and low merger vote fraction samples is their UV sizes as measured by  $r_{50}$ . Here, we explore potential reasons for this difference and implications for the nature of LyC-emitters.

On Figure 8 we show the position of mergers and low vote fraction mergers in the mass-size diagram, with markers color-coded by the fraction of votes going to merger categories. One may notice that the bulk of galaxies with low merger vote fractions tend to reside in the low-mass ( $M_* < 10^9 M_\odot$ ), small angular size ( $r_{80} < 0.3''$ ) corner of the diagram. Interestingly, when examining the merger stages of low merger vote fraction galaxies, we find that when they are voted as mergers, they are consistently identified as post-coalescence galaxies (see Figure 1).

The classification of mergers is generally challenging, and citizen science experiments have shown that even clear galaxy mergers tend to have low merger vote fractions (Lintott et al. 2008; Darg et al. 2010). Most galaxies identified in LaCOS may be at post-interaction and pre-coalescence stages, simply because those are the easiest stages to identify visually with certainty, since they present both separate nuclei and tidal features. Therefore, we may expect some of the more compact galaxies in LaCOS to also be mergers, and the merger fractions in LaCOS to be larger than the values derived with our identification scheme. Yet, it is extremely difficult to ascertain which of the galaxies with low merger vote fraction are or are not mergers solely with the HST imaging presented here. Deeper observations could potentially reveal fainter isophotes, and dedicated morphometrics

or CNN calibrations adapted to the galaxy property parameter space and specificity of the survey could help refine the identification process. However, and given the data currently at hand, the LaCOS visual merger fractions provide the best lower limits achievable at this stage.

Therefore, two possible options emerge regarding the nature of the objects with low merger vote fraction. The first is that those objects are low-mass, compact star-forming galaxies where stellar feedback is sufficient to allow LyC escape. Simulations have shown that stellar feedback alone can significantly perturb the neutral gas medium in low-mass galaxies, due to their shallow gravitational potential wells (Rey et al. 2022; Trebitsch et al. 2017, e.g.). The interplay between star-formation and feedback in dwarf galaxies has been proposed to drive episodic increase in star-formation, in a so-called "breathing mode" (Stinson et al. 2007; Muratov et al. 2015). In this paradigm, low-mass galaxies go through a starburst cycle that starts with an initial star-forming episode. The newly formed stars lead to both stellar, and eventually, supernova feedback, that expel the gas due to the shallow potential wells, and temporarily stops star formation. As the gas is re-accreted, star formation starts anew and the cycle continues. Cenci et al. (2024) have shown that star formation bursts in simulated galaxies are driven by central gas compaction events, and that the mechanisms responsible for those can be split in two categories. On the one side, merger interactions drive gas compaction and starburst events for most high-mass galaxies ( $M_* > 10^{10} M_\odot$ ), and are also responsible for the most intense and long-lived starbursts at low-mass ( $M_* \sim 10^8 - 10^{10} M_\odot$ ) (Cenci et al. 2024). On the other side, a significant fraction of starbursting low-mass galaxies (40-50%) are not undergoing interactions, and instead have bursts occurring due to their star-formation breathing mode (Cenci et al. 2024). Therefore, galaxy mergers may play a major role in facilitating LyC escape mainly from larger-mass galaxies, where feedback alone is not sufficient to clear the neutral interstellar medium. We note similar conclusions have been reached for the role of mergers in Ly $\alpha$ -emission (Le Reste et al. 2025b; Ren et al. 2025). Additionally, this dichotomy of mechanisms, and in particular the breathing-mode of star formation in low-mass galaxies is in agreement with the Flury et al. (2022a) interpretation of LyC measurements as a duty cycle and the Flury et al. (2025) finding that bursty star formation is associated with LyC escape.

Another interpretation may be that some of the compact low-mass galaxies with low merger vote fractions in LaCOS are in fact mergers at coalescence, where the

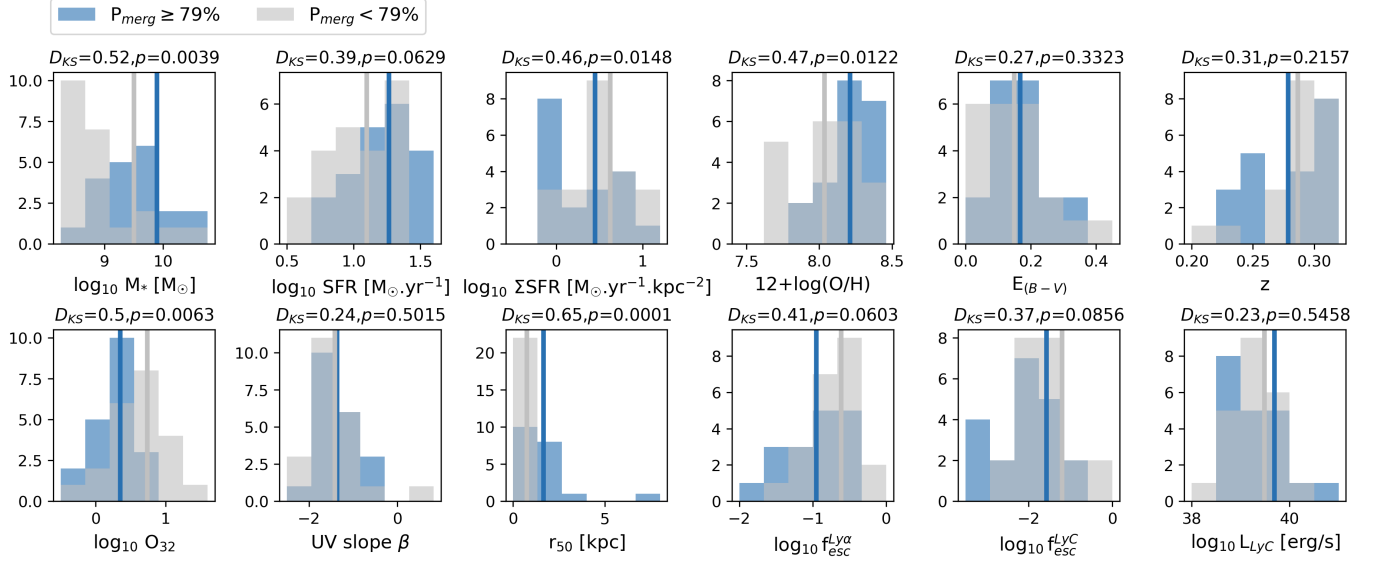


**Figure 7.** Histograms of various galaxy properties for LaCOS galaxies with  $P_{\text{merg}} \geq 79\%$  (blue) and  $P_{\text{merg}} < 79\%$  (gray). Vertical lines show the mean for each sample. The K-S test distance statistic and associated  $p$ -value for the two samples are shown above each histogram. The robustly identified mergers have properties generally consistent with those of galaxies with low merger vote fractions ( $p > 0.05$ ), with the notable exception of  $r_{50}$ . Robust galaxy mergers have significantly larger radii than their low merger vote fraction counterparts.

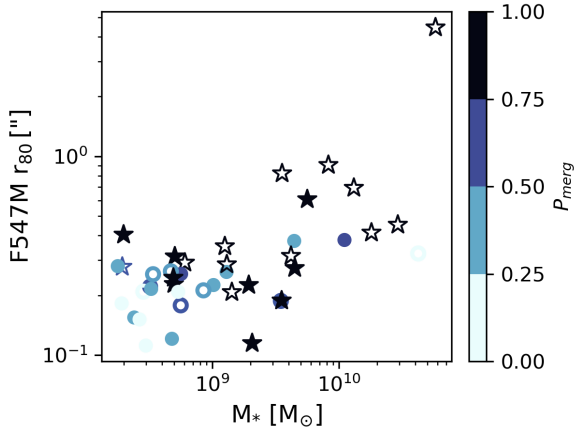


**Figure 8.** Radius containing 80% of the light in the F547M filter (similar to rest-frame B-band) as a function of the stellar mass, color-coded by the merger vote fraction. Star markers show galaxies with  $P_{\text{merg}} \geq 79\%$ , circle markers show galaxies with  $P_{\text{merg}} < 79\%$ . Markers are filled if the galaxy is a LyC-emitter, they are empty otherwise. Compact and low-mass galaxies tend to be voted as mergers less often than massive, extended galaxies in LaCOS.

SFR enhancement is the highest (Ferreira et al. 2025). Low-mass merging galaxies are harder to identify than their higher-mass counterparts, and discerning low-mass mergers at coalescence may be even more difficult. The progenitors of low-mass coalescing systems are likely to have even lower masses  $M_* < 10^7 M_\odot$ , so that such an interaction would result in extremely faint stellar tidal features. However, since low-mass galaxies are gas-

dominated, a potential avenue would be to observe their neutral gas distributions. While the breathing mode of star-formation is expected to yield quasi-isotropic gas outflows (Cenci et al. 2024), mergers result in highly anisotropic and asymmetric gas distributions, that can be probed using the asymmetry applied to 21cm maps (Holwerda et al. 2011, 2025). 21cm Hi interferometric observations of galaxies analogous to the high- $z$  population, such as green peas and Ly $\alpha$ -emitters, have shown that galaxy interactions may be common in those populations (Purkayastha et al. 2022, 2024; Dutta et al. 2024; Le Reste et al. 2025b). While 21cm interferometric observations have so far remained mostly limited to the very local Universe ( $z < 0.05$ ) where LyC cannot be observed easily due to the low throughput of observation, the SKA is set to observe galaxies in 21cm up to  $z \sim 1$  (Staveley-Smith & Oosterloo 2015). Those observations will make the accurate detection of gas-dominated, low-mass mergers feasible at higher redshifts than possible before in the near-future, and thus help the characterization of low-mass, compact, extremely star-forming galaxies.

## 5.2. Implications for merger-driven LyC emission at reionization

While we have shown galaxy mergers account for  $\geq 41\%$  of LyC-emitters in LaCOS, and can thus lead to LyC production and escape in the low- $z$  Universe, ultimately we want to determine whether this mechanism could apply at high- $z$ , and specifically at the Epoch of

Reionization. As already mentioned, mergers are notoriously difficult to detect at high- $z$ , but James Webb Space Telescope observations have recently opened the way to the characterization of mergers in the early Universe. An initial study using morphometrics criteria developed for high-mass, low- $z$  galaxies found that the merger fraction did not evolve with redshift, and merging galaxies did not have properties significantly different from non-mergers (Dalmasso et al. 2024). Additionally, another study using  $f_{esc}^{LyC}$  calibrations derived from  $z \sim 0$  samples and merger identification through morphometrics criteria developed at  $z \sim 1$  applied to rest-frame UV JWST imaging concluded mergers represent a small fraction of galaxies with high  $f_{esc}^{LyC}$  predictions at  $z = 5 - 7$  (Mascia et al. 2025). However, simulations have shown that the use of morphometrics to identify mergers is limited at  $z > 2$  (Abruzzo et al. 2018) and as illustrated in Appendix B, morphometrics merger calibrations are specific to the galaxy population and survey considered, likely yielding low accuracy classifications at the Epoch of Reionization. In fact, the results in Mascia et al. (2025) are in agreement with ours, and show that predicted LyC-emitters tend to have low asymmetry in the UV, which is also found in LaCOS. Therefore, the type of objects likely to emit LyC emission, i.e. galaxies with compact, unobscured UV regions and in the case of mergers, systems close to coalescence, might not change drastically with redshift.

Recently, new approaches based on probabilistic photometric pair detection have brought insights onto the evolution of merger properties up to  $z = 11$  (Duan et al. 2024, 2025). Those studies have found that the merger fraction increases with redshift up to  $z = 8$ , and that the merger rate increases up to  $z \sim 6$ , after which it flattens. Specifically, a typical galaxy at the Epoch of Reionization will experience on average 6 merger events per Gyr, but merger timescales, while difficult to establish, are also thought to be shorter at high-redshift ( $\sim 100$  Myr at  $z \sim 6$ ) (Duan et al. 2025). The star formation rate of pair galaxies is similar to that of isolated objects, except for very small separations ( $< 20$  kpc), where pairs show a small enhancement in SFR (Duan et al. 2024). Thus, enhancements in  $f_{esc}^{LyC}$  linked to heightened star-forming activity during interactions may happen on a shorter timescale at reionization than they do in the low- $z$  Universe. However, galaxy pairs show an AGN excess as compared to non interacting galaxies (Duan et al. 2024), which could also potentially play a role in reionization, as AGNs could contribute a fraction of the ionizing photons at  $z > 6$  (Dayal et al. 2020; Trebitsch et al. 2023). Definitive conclusions on LyC emission from mergers at the Epoch of Reionization will require

additional work on the LyC properties of galaxy mergers, and their evolution with redshift. In particular, here we have measured the merger fraction among LyC candidates in LaCOS, but the specific criteria used to select galaxies for LyC observations limit range of merger properties probed. To fully assess the role of mergers in LyC emission, surveys targeting the ionizing properties of large samples of merging galaxies - particularly those extending to low stellar masses and including AGNs - will be necessary. Combining measurements from such surveys with merger statistics at  $z > 5$ , would allow the estimation of the total ionizing photon contribution from galaxy mergers during the Epoch of Reionization.

## 6. CONCLUSION

We have characterized the morphology and merger properties of LyC-emitting galaxies and candidates using rest-frame optical and UV HST imaging from the LaCOS survey (Le Reste et al. 2025a), which imaged 42 galaxies observed in LyC from the LzLCS survey (Flury et al. 2022b). We find that:

1. Lyman Continuum emitting galaxies tend to be compact, both in rest-frame UV and optical bands. While the selection criteria used to select galaxies for LyC observations, in particular large  $\Sigma SFR$  might contribute to this trend, we find robust anti-correlations between  $f_{esc}^{LyC}$  and radii ( $r_{20}$ ,  $r_{50}$  and  $r_{80}$ ) in almost all bands sampled by LaCOS photometry. We also find strong anti-correlations between the asymmetry, the clumpiness and  $f_{esc}^{LyC}$  in the bluest LaCOS filter available (F150LP). We derive fits between robustly anti-correlated morphometrics and  $f_{esc}^{LyC}$ , with a characteristic scatter of  $\sim 0.3$  dex. We interpret these results as due to LyC photons escaping more easily in compact star-forming galaxies with a small number of centrally-concentrated UV clusters, in agreement with results from other studies using LaCOS data (Le Reste et al. 2025a; Saldana-Lopez et al. 2025).
2. Both LyC-emitting galaxy samples and samples selected as LyC candidates through properties associated with high  $f_{esc}^{LyC}$  (high  $O_{32}$ ,  $\Sigma SFR$  or small UV  $\beta$  slopes) at  $z \sim 0.3$  have high merger fractions. Specifically, we find that  $\geq 48\%$  of LaCOS galaxies and  $\geq 41\%$  of LaCOS LyC-emitters are galaxy mergers. We do not find statistically significant differences between the  $f_{esc}^{LyC}$  properties of robustly identified mergers and galaxies with low merger vote fractions ( $P_{merg} < 79\%$ , equivalent to a  $< 3\sigma$  confidence merger classification).

3. The galaxy mergers confidently identified in LACOS are all at advanced stages of interaction (i.e., visually classified as post-interaction or near coalescence), having undergone at least one pericenter passage, and with a median projected separation of 1.4 kpc. LyC-emitting and non-emitting mergers have similar merger stage distributions. The range in merger stages is too small to robustly evaluate the impact of merger advancement on  $f_{esc}^{LyC}$ , but our results could indicate that LyC emission during merger interactions happens within a narrow time window ( $\lesssim$  few 100 Myr) at the end of the interaction.

Here, we have presented the most robust estimates to date of the merger fractions in a sample of LyC-emitting galaxies, and have characterized the properties of the identified mergers. While these results offer valuable insight into the connection between galaxy interactions and LyC escape, the classification of mergers remains intrinsically challenging, and the criteria used to select our sample limit inferences on the role mergers play in facilitating LyC emission. Moving forward, dedicated multi-wavelength surveys targeting mergers across a broad dynamical range will be crucial to improve estimates of the merger timescales and configurations during which LyC leakage is most likely to occur. Notably, 21cm HI emission mapping of galaxies selected through  $f_{esc}^{LyC}$  calibrations at lower redshifts would significantly enhance classification accuracy by identifying post-coalescence, compact mergers likely to be missed in optical and UV imaging. New and upcoming facilities such as Euclid, the SKA, Roman, and the Habitable Worlds Observatory will be instrumental in solving the role of mergers

on LyC emission. When combined with detailed merger properties at  $z > 5$ , these data will enable a comprehensive evaluation of the contribution of galaxy mergers to the Epoch of Reionization.

## 7. DATA AVAILABILITY

The HST data used for the analysis in this manuscript is publicly released at the Barbara A. Mikulski Archive for Space Telescopes (MAST) as a High Level Science Product, with DOI: 10.17909/j4qd-ev76, accessible via <https://archive.stsci.edu/hlsp/lacos/>.

This research is based on observations made with the NASA/ESA Hubble Space Telescope obtained from the Space Telescope Science Institute, which is operated by the Association of Universities for Research in Astronomy, Inc., under NASA contract NAS 5-26555. These observations are associated with HST GO programs 17069, 14131 and 11107. This research has made use of the NASA/IPAC Infrared Science Archive, which is funded by the National Aeronautics and Space Administration and operated by the California Institute of Technology. ALR and MSO acknowledge support from HST GO-17069.

*Software:* numpy (Harris et al. 2020), astropy (Astropy Collaboration et al. 2013, 2018, 2022), matplotlib (Hunter 2007), photutils (Bradley et al. 2024), scipy (Virtanen et al. 2020), statmorph (Rodríguez-Gómez et al. 2019), linmix (Kelly 2007), sep (Barbary 2016), histogram (Flury et al. 2022b), KaplanMeier (Flury et al. 2024).

*Facilities:* HST,IRSA

## REFERENCES

- Abraham, R. G., Valdes, F., Yee, H. K. C., & van den Bergh, S. 1994, ApJ, 432, 75, doi: [10.1086/174550](https://doi.org/10.1086/174550)
- Abraham, R. G., van den Bergh, S., Glazebrook, K., et al. 1996, ApJS, 107, 1, doi: [10.1086/192352](https://doi.org/10.1086/192352)
- Abraham, R. G., van den Bergh, S., & Nair, P. 2003, ApJ, 588, 218, doi: [10.1086/373919](https://doi.org/10.1086/373919)
- Abruzzo, M. W., Narayanan, D., Davé, R., & Thompson, R. 2018, arXiv e-prints, arXiv:1803.02374, doi: [10.48550/arXiv.1803.02374](https://doi.org/10.48550/arXiv.1803.02374)
- Allam, S. S., Tucker, D. L., Smith, J. A., et al. 2004, AJ, 127, 1883, doi: [10.1086/381954](https://doi.org/10.1086/381954)
- Amorín, R. O., Rodríguez-Henríquez, M., Fernández, V., et al. 2024, A&A, 682, L25, doi: [10.1051/0004-6361/202449175](https://doi.org/10.1051/0004-6361/202449175)
- Astropy Collaboration, Robitaille, T. P., Tollerud, E. J., et al. 2013, A&A, 558, A33, doi: [10.1051/0004-6361/201322068](https://doi.org/10.1051/0004-6361/201322068)
- Astropy Collaboration, Price-Whelan, A. M., Sipőcz, B. M., et al. 2018, AJ, 156, 123, doi: [10.3847/1538-3881/aabc4f](https://doi.org/10.3847/1538-3881/aabc4f)
- Astropy Collaboration, Price-Whelan, A. M., Lim, P. L., et al. 2022, ApJ, 935, 167, doi: [10.3847/1538-4357/ac7c74](https://doi.org/10.3847/1538-4357/ac7c74)
- Bait, O., Borthakur, S., Schaerer, D., et al. 2024, A&A, 688, A198, doi: [10.1051/0004-6361/202348416](https://doi.org/10.1051/0004-6361/202348416)
- Barbary, K. 2016, The Journal of Open Source Software, 1, 58, doi: [10.21105/joss.00058](https://doi.org/10.21105/joss.00058)
- Barrow, K. S. S., Robertson, B. E., Ellis, R. S., et al. 2020, ApJL, 902, L39, doi: [10.3847/2041-8213/abbd8e](https://doi.org/10.3847/2041-8213/abbd8e)



- Begley, R., Cullen, F., McLure, R. J., et al. 2022, *MNRAS*, 513, 3510, doi: [10.1093/mnras/stac1067](https://doi.org/10.1093/mnras/stac1067)
- . 2024, *MNRAS*, 527, 4040, doi: [10.1093/mnras/stad3417](https://doi.org/10.1093/mnras/stad3417)
- Bergvall, N., Leitert, E., Zackrisson, E., & Marquart, T. 2013, *A&A*, 554, A38, doi: [10.1051/0004-6361/201118433](https://doi.org/10.1051/0004-6361/201118433)
- Bershady, M. A., Jangren, A., & Conselice, C. J. 2000, *AJ*, 119, 2645, doi: [10.1086/301386](https://doi.org/10.1086/301386)
- Bertin, E., & Arnouts, S. 1996, *A&AS*, 117, 393, doi: [10.1051/aas:1996164](https://doi.org/10.1051/aas:1996164)
- Bickley, R. W., Wilkinson, S., Ferreira, L., et al. 2024, *MNRAS*, 534, 2533, doi: [10.1093/mnras/stae2246](https://doi.org/10.1093/mnras/stae2246)
- Bradley, L., Sipőcz, B., Robitaille, T., et al. 2024, *astropy/photutils*: 2.0.2, 2.0.2, Zenodo, doi: [10.5281/zenodo.13989456](https://doi.org/10.5281/zenodo.13989456)
- Bridge, C. R., Teplitz, H. I., Siana, B., et al. 2010, *ApJ*, 720, 465, doi: [10.1088/0004-637X/720/1/465](https://doi.org/10.1088/0004-637X/720/1/465)
- Carr, C. A., Cen, R., Scarlata, C., et al. 2025, *ApJ*, 982, 137, doi: [10.3847/1538-4357/adb72f](https://doi.org/10.3847/1538-4357/adb72f)
- Cenci, E., Feldmann, R., Gensior, J., et al. 2024, *MNRAS*, 527, 7871, doi: [10.1093/mnras/stad3709](https://doi.org/10.1093/mnras/stad3709)
- Chisholm, J., Orlitová, I., Schaerer, D., et al. 2017, *A&A*, 605, A67, doi: [10.1051/0004-6361/201730610](https://doi.org/10.1051/0004-6361/201730610)
- Chisholm, J., Gazagnes, S., Schaerer, D., et al. 2018, *A&A*, 616, A30, doi: [10.1051/0004-6361/201832758](https://doi.org/10.1051/0004-6361/201832758)
- Chisholm, J., Saldana-Lopez, A., Flury, S., et al. 2022, *MNRAS*, 517, 5104, doi: [10.1093/mnras/stac2874](https://doi.org/10.1093/mnras/stac2874)
- Choustikov, N., Katz, H., Saxena, A., et al. 2024, *MNRAS*, 529, 3751, doi: [10.1093/mnras/stae776](https://doi.org/10.1093/mnras/stae776)
- Conselice, C. J. 2003, *ApJS*, 147, 1, doi: [10.1086/375001](https://doi.org/10.1086/375001)
- Conselice, C. J., Bershady, M. A., & Jangren, A. 2000, *ApJ*, 529, 886, doi: [10.1086/308300](https://doi.org/10.1086/308300)
- Conselice, C. J., Yang, C., & Bluck, A. F. L. 2009, *MNRAS*, 394, 1956, doi: [10.1111/j.1365-2966.2009.14396.x](https://doi.org/10.1111/j.1365-2966.2009.14396.x)
- Cristiani, S., Serrano, L. M., Fontanot, F., Vanzella, E., & Monaco, P. 2016, *MNRAS*, 462, 2478, doi: [10.1093/mnras/stw1810](https://doi.org/10.1093/mnras/stw1810)
- Dalmasso, N., Calabrò, A., Leethochawalit, N., et al. 2024, *MNRAS*, 533, 4472, doi: [10.1093/mnras/stae2064](https://doi.org/10.1093/mnras/stae2064)
- Darg, D. W., Kaviraj, S., Lintott, C. J., et al. 2010, *MNRAS*, 401, 1043, doi: [10.1111/j.1365-2966.2009.15686.x](https://doi.org/10.1111/j.1365-2966.2009.15686.x)
- Dayal, P., Volonteri, M., Choudhury, T. R., et al. 2020, *MNRAS*, 495, 3065, doi: [10.1093/mnras/staa1138](https://doi.org/10.1093/mnras/staa1138)
- Domínguez Sánchez, H., Martin, G., Damjanov, I., et al. 2023, *MNRAS*, 521, 3861, doi: [10.1093/mnras/stad750](https://doi.org/10.1093/mnras/stad750)
- Duan, Q., Li, Q., Conselice, C. J., et al. 2024, *arXiv e-prints*, arXiv:2411.04944, doi: [10.48550/arXiv.2411.04944](https://doi.org/10.48550/arXiv.2411.04944)
- Duan, Q., Conselice, C. J., Li, Q., et al. 2025, *MNRAS*, 540, 774, doi: [10.1093/mnras/staf638](https://doi.org/10.1093/mnras/staf638)
- Duncan, K., Conselice, C. J., Mundy, C., et al. 2019, *ApJ*, 876, 110, doi: [10.3847/1538-4357/ab148a](https://doi.org/10.3847/1538-4357/ab148a)
- Dutta, S., Bera, A., Bait, O., et al. 2024, *MNRAS*, 531, 5140, doi: [10.1093/mnras/stae1490](https://doi.org/10.1093/mnras/stae1490)
- Ejdetjärn, T., Agertz, O., Renaud, F., et al. 2025, *arXiv e-prints*, arXiv:2503.01982, doi: [10.48550/arXiv.2503.01982](https://doi.org/10.48550/arXiv.2503.01982)
- Elmegreen, B. G., Elmegreen, D. M., & Montenegro, L. 1992, *ApJS*, 79, 37, doi: [10.1086/191643](https://doi.org/10.1086/191643)
- Faria, L., Patton, D. R., Courteau, S., Ellison, S., & Brown, W. 2025, *MNRAS*, 537, 915, doi: [10.1093/mnras/staf124](https://doi.org/10.1093/mnras/staf124)
- Ferreira, L., Conselice, C. J., Duncan, K., et al. 2020, *ApJ*, 895, 115, doi: [10.3847/1538-4357/ab8f9b](https://doi.org/10.3847/1538-4357/ab8f9b)
- Ferreira, L., Ellison, S. L., Patton, D. R., et al. 2025, *MNRAS*, 538, L31, doi: [10.1093/mnrasl/slaf004](https://doi.org/10.1093/mnrasl/slaf004)
- Finkelstein, S. L., D'Aloisio, A., Paardekooper, J.-P., et al. 2019, *ApJ*, 879, 36, doi: [10.3847/1538-4357/ab1ea8](https://doi.org/10.3847/1538-4357/ab1ea8)
- Fletcher, T. J., Tang, M., Robertson, B. E., et al. 2019, *ApJ*, 878, 87, doi: [10.3847/1538-4357/ab2045](https://doi.org/10.3847/1538-4357/ab2045)
- Flury, S. R., Jaskot, A. E., Ferguson, H. C., et al. 2022a, *ApJ*, 930, 126, doi: [10.3847/1538-4357/ac61e4](https://doi.org/10.3847/1538-4357/ac61e4)
- . 2022b, *ApJS*, 260, 1, doi: [10.3847/1538-4365/ac5331](https://doi.org/10.3847/1538-4365/ac5331)
- Flury, S. R., Jaskot, A. E., Saldana-Lopez, A., et al. 2024, *arXiv e-prints*, arXiv:2409.12118, doi: [10.48550/arXiv.2409.12118](https://doi.org/10.48550/arXiv.2409.12118)
- . 2025, *ApJ*, 985, 128, doi: [10.3847/1538-4357/adc305](https://doi.org/10.3847/1538-4357/adc305)
- Freeman, P. E., Izbicki, R., Lee, A. B., et al. 2013, *MNRAS*, 434, 282, doi: [10.1093/mnras/stt1016](https://doi.org/10.1093/mnras/stt1016)
- Gazagnes, S., Chisholm, J., Schaerer, D., Verhamme, A., & Izotov, Y. 2020, *A&A*, 639, A85, doi: [10.1051/0004-6361/202038096](https://doi.org/10.1051/0004-6361/202038096)
- Gazagnes, S., Chisholm, J., Schaerer, D., et al. 2018, *A&A*, 616, A29, doi: [10.1051/0004-6361/201832759](https://doi.org/10.1051/0004-6361/201832759)
- Giovinazzo, E., Oesch, P. A., Weibel, A., et al. 2025, *arXiv e-prints*, arXiv:2507.01096, doi: [10.48550/arXiv.2507.01096](https://doi.org/10.48550/arXiv.2507.01096)
- Grazian, A., Giallongo, E., Boutsia, K., et al. 2018, *A&A*, 613, A44, doi: [10.1051/0004-6361/201732385](https://doi.org/10.1051/0004-6361/201732385)
- . 2024, *ApJ*, 974, 84, doi: [10.3847/1538-4357/ad6980](https://doi.org/10.3847/1538-4357/ad6980)
- Guo, Y., Ferguson, H. C., Bell, E. F., et al. 2015, *ApJ*, 800, 39, doi: [10.1088/0004-637X/800/1/39](https://doi.org/10.1088/0004-637X/800/1/39)
- Gupta, A., Trott, C. M., Jaiswar, R., et al. 2024, *ApJ*, 973, 169, doi: [10.3847/1538-4357/ad6767](https://doi.org/10.3847/1538-4357/ad6767)
- Harikane, Y., Zhang, Y., Nakajima, K., et al. 2023, *ApJ*, 959, 39, doi: [10.3847/1538-4357/ad029e](https://doi.org/10.3847/1538-4357/ad029e)
- Harris, C. R., Millman, K. J., van der Walt, S. J., et al. 2020, *Nature*, 585, 357, doi: [10.1038/s41586-020-2649-2](https://doi.org/10.1038/s41586-020-2649-2)
- Hassan, S., Davé, R., Mitra, S., et al. 2018, *MNRAS*, 473, 227, doi: [10.1093/mnras/stx2194](https://doi.org/10.1093/mnras/stx2194)

- Heckman, T. M., Borthakur, S., Overzier, R., et al. 2011, *ApJ*, 730, 5, doi: [10.1088/0004-637X/730/1/5](https://doi.org/10.1088/0004-637X/730/1/5)
- Herenz, E. C., Schaible, A., Laursen, P., et al. 2025, *A&A*, 693, A252, doi: [10.1051/0004-6361/202451012](https://doi.org/10.1051/0004-6361/202451012)
- Holmberg, E. 1941, *ApJ*, 94, 385, doi: [10.1086/144344](https://doi.org/10.1086/144344)
- Holwerda, B. W., Pirzkal, N., Cox, T. J., et al. 2011, *MNRAS*, 416, 2426, doi: [10.1111/j.1365-2966.2011.18940.x](https://doi.org/10.1111/j.1365-2966.2011.18940.x)
- Holwerda, B. W., Dénes, H., Rhee, J., et al. 2025, *PASA*, 42, e028, doi: [10.1017/pasa.2025.5](https://doi.org/10.1017/pasa.2025.5)
- Hunter, J. D. 2007, *Computing in Science & Engineering*, 9, 90, doi: [10.1109/MCSE.2007.55](https://doi.org/10.1109/MCSE.2007.55)
- Inoue, A. K., Shimizu, I., Iwata, I., & Tanaka, M. 2014, *MNRAS*, 442, 1805, doi: [10.1093/mnras/stu936](https://doi.org/10.1093/mnras/stu936)
- Isobe, T., Feigelson, E. D., & Nelson, P. I. 1986, *ApJ*, 306, 490, doi: [10.1086/164359](https://doi.org/10.1086/164359)
- Izotov, Y. I., Chisholm, J., Worseck, G., et al. 2022, *MNRAS*, 515, 2864, doi: [10.1093/mnras/stac1899](https://doi.org/10.1093/mnras/stac1899)
- Izotov, Y. I., Schaerer, D., Thuan, T. X., et al. 2016, *MNRAS*, 461, 3683, doi: [10.1093/mnras/stw1205](https://doi.org/10.1093/mnras/stw1205)
- Izotov, Y. I., Worseck, G., Schaerer, D., et al. 2021, *MNRAS*, 503, 1734, doi: [10.1093/mnras/stab612](https://doi.org/10.1093/mnras/stab612)
- . 2018, *MNRAS*, 478, 4851, doi: [10.1093/mnras/sty1378](https://doi.org/10.1093/mnras/sty1378)
- Jaskot, A. E. 2025, *Annual Review of Astronomy and Astrophysics*, doi: <https://doi.org/10.1146/annurev-astro-111324-074935>
- Jaskot, A. E., Oey, M. S., Scarlata, C., & Dowd, T. 2017, *ApJL*, 851, L9, doi: [10.3847/2041-8213/aa9d83](https://doi.org/10.3847/2041-8213/aa9d83)
- Jaskot, A. E., Silveyra, A. C., Plantinga, A., et al. 2024, arXiv e-prints, arXiv:2406.10171, doi: [10.48550/arXiv.2406.10171](https://doi.org/10.48550/arXiv.2406.10171)
- Ji, Z., Giallisco, M., Vanzella, E., et al. 2020, *ApJ*, 888, 109, doi: [10.3847/1538-4357/ab5fdc](https://doi.org/10.3847/1538-4357/ab5fdc)
- Ji, Z., Alberts, S., Zhu, Y., et al. 2025, arXiv e-prints, arXiv:2504.01067, doi: [10.48550/arXiv.2504.01067](https://doi.org/10.48550/arXiv.2504.01067)
- Kartaltepe, J. S., Mozena, M., Kocevski, D., et al. 2015, *ApJS*, 221, 11, doi: [10.1088/0067-0049/221/1/11](https://doi.org/10.1088/0067-0049/221/1/11)
- Kaviraj, S., Devriendt, J., Dubois, Y., et al. 2015, *MNRAS*, 452, 2845, doi: [10.1093/mnras/stv1500](https://doi.org/10.1093/mnras/stv1500)
- Kelly, B. C. 2007, *ApJ*, 665, 1489, doi: [10.1086/519947](https://doi.org/10.1086/519947)
- Kent, S. M. 1985, *ApJS*, 59, 115, doi: [10.1086/191066](https://doi.org/10.1086/191066)
- Khostovan, A. A., Kartaltepe, J. S., Salvato, M., et al. 2025, arXiv e-prints, arXiv:2503.00120, doi: [10.48550/arXiv.2503.00120](https://doi.org/10.48550/arXiv.2503.00120)
- Kim, K. J., Bayliss, M. B., Rigby, J. R., et al. 2023, *ApJL*, 955, L17, doi: [10.3847/2041-8213/acf0c5](https://doi.org/10.3847/2041-8213/acf0c5)
- Komarova, L., Oey, M. S., Krumholz, M. R., et al. 2021, *ApJL*, 920, L46, doi: [10.3847/2041-8213/ac2c09](https://doi.org/10.3847/2041-8213/ac2c09)
- Komarova, L., Oey, M. S., Hernandez, S., et al. 2024, *ApJ*, 967, 117, doi: [10.3847/1538-4357/ad3962](https://doi.org/10.3847/1538-4357/ad3962)
- Komarova, L., Oey, S., Marques-Chaves, R., et al. 2025, arXiv e-prints, arXiv:2506.19623, doi: [10.48550/arXiv.2506.19623](https://doi.org/10.48550/arXiv.2506.19623)
- Kostyuk, I., & Ciardi, B. 2024, arXiv e-prints, arXiv:2412.04348. <https://arxiv.org/abs/2412.04348>
- Kreilgaard, K. C., Mason, C. A., Cullen, F., Begley, R., & McLure, R. J. 2024, *A&A*, 692, A57, doi: [10.1051/0004-6361/202450747](https://doi.org/10.1051/0004-6361/202450747)
- Le Fèvre, O., Abraham, R., Lilly, S. J., et al. 2000, *MNRAS*, 311, 565, doi: [10.1046/j.1365-8711.2000.03083.x](https://doi.org/10.1046/j.1365-8711.2000.03083.x)
- Le Reste, A., Cannon, J. M., Hayes, M. J., et al. 2024, *MNRAS*, 528, 757, doi: [10.1093/mnras/stad3910](https://doi.org/10.1093/mnras/stad3910)
- Le Reste, A., Scarlata, C., Hayes, M., et al. 2025a, arXiv e-prints, arXiv:2504.07056, doi: [10.48550/arXiv.2504.07056](https://doi.org/10.48550/arXiv.2504.07056)
- Le Reste, A., Hayes, M. J., Cannon, J. M., et al. 2025b, *A&A*, 693, A253, doi: [10.1051/0004-6361/202452034](https://doi.org/10.1051/0004-6361/202452034)
- Leclercq, F., Chisholm, J., King, W., et al. 2024, *A&A*, 687, A73, doi: [10.1051/0004-6361/202449362](https://doi.org/10.1051/0004-6361/202449362)
- Leitet, E., Bergvall, N., Hayes, M., Linné, S., & Zackrisson, E. 2013, *A&A*, 553, A106, doi: [10.1051/0004-6361/201118370](https://doi.org/10.1051/0004-6361/201118370)
- Lin, Y.-H., Scarlata, C., Williams, H., et al. 2024, *MNRAS*, 527, 4173, doi: [10.1093/mnras/stad3483](https://doi.org/10.1093/mnras/stad3483)
- Lintott, C. J., Schawinski, K., Slosar, A., et al. 2008, *MNRAS*, 389, 1179, doi: [10.1111/j.1365-2966.2008.13689.x](https://doi.org/10.1111/j.1365-2966.2008.13689.x)
- Lotz, J. M., Jonsson, P., Cox, T. J., & Primack, J. R. 2008, *MNRAS*, 391, 1137, doi: [10.1111/j.1365-2966.2008.14004.x](https://doi.org/10.1111/j.1365-2966.2008.14004.x)
- Lotz, J. M., Primack, J., & Madau, P. 2004, *AJ*, 128, 163, doi: [10.1086/421849](https://doi.org/10.1086/421849)
- Ma, X., Quataert, E., Wetzel, A., et al. 2020, *MNRAS*, 498, 2001, doi: [10.1093/mnras/staa2404](https://doi.org/10.1093/mnras/staa2404)
- Madau, P., Giallongo, E., Grazian, A., & Haardt, F. 2024, *ApJ*, 971, 75, doi: [10.3847/1538-4357/ad5ce8](https://doi.org/10.3847/1538-4357/ad5ce8)
- Mager, V. A., Conselice, C. J., Seibert, M., et al. 2018, *ApJ*, 864, 123, doi: [10.3847/1538-4357/aad59e](https://doi.org/10.3847/1538-4357/aad59e)
- Marques-Chaves, R., Schaerer, D., Álvarez-Márquez, J., et al. 2021, *MNRAS*, 507, 524, doi: [10.1093/mnras/stab2187](https://doi.org/10.1093/mnras/stab2187)
- Marques-Chaves, R., Schaerer, D., Vanzella, E., et al. 2024, *A&A*, 691, A87, doi: [10.1051/0004-6361/202451667](https://doi.org/10.1051/0004-6361/202451667)
- Martin, C. L., Peng, Z., & Li, Y. 2024, *ApJ*, 966, 190, doi: [10.3847/1538-4357/ad34ac](https://doi.org/10.3847/1538-4357/ad34ac)
- Mascia, S., Pentericci, L., Calabrò, A., et al. 2024, *A&A*, 685, A3, doi: [10.1051/0004-6361/202347884](https://doi.org/10.1051/0004-6361/202347884)
- Mascia, S., Pentericci, L., Llerena, M., et al. 2025, arXiv e-prints, arXiv:2501.08268, doi: [10.48550/arXiv.2501.08268](https://doi.org/10.48550/arXiv.2501.08268)

- Matsuoka, Y., Onoue, M., Iwasawa, K., et al. 2023, *ApJL*, 949, L42, doi: [10.3847/2041-8213/acd69f](https://doi.org/10.3847/2041-8213/acd69f)
- Maulick, S., Saha, K., Kataria, M., & Herenz, E. C. 2024, *ApJ*, 972, 138, doi: [10.3847/1538-4357/ad6155](https://doi.org/10.3847/1538-4357/ad6155)
- Micheva, G., Iwata, I., & Inoue, A. K. 2017, *MNRAS*, 465, 302, doi: [10.1093/mnras/stw1329](https://doi.org/10.1093/mnras/stw1329)
- Morgan, W. W. 1958, *PASP*, 70, 364, doi: [10.1086/127243](https://doi.org/10.1086/127243)
- Mostardi, R. E., Shapley, A. E., Steidel, C. C., et al. 2015, *ApJ*, 810, 107, doi: [10.1088/0004-637X/810/2/107](https://doi.org/10.1088/0004-637X/810/2/107)
- Muratov, A. L., Kereš, D., Faucher-Giguère, C.-A., et al. 2015, *MNRAS*, 454, 2691, doi: [10.1093/mnras/stv2126](https://doi.org/10.1093/mnras/stv2126)
- Naidu, R. P., Tacchella, S., Mason, C. A., et al. 2020, *ApJ*, 892, 109, doi: [10.3847/1538-4357/ab7cc9](https://doi.org/10.3847/1538-4357/ab7cc9)
- Nakajima, K., Ellis, R. S., Robertson, B. E., Tang, M., & Stark, D. P. 2020, *ApJ*, 889, 161, doi: [10.3847/1538-4357/ab6604](https://doi.org/10.3847/1538-4357/ab6604)
- Pahl, A. J., Shapley, A., Steidel, C. C., Chen, Y., & Reddy, N. A. 2021, *MNRAS*, 505, 2447, doi: [10.1093/mnras/stab1374](https://doi.org/10.1093/mnras/stab1374)
- Pan, H.-A., Lin, L., Hsieh, B.-C., et al. 2019, *ApJ*, 881, 119, doi: [10.3847/1538-4357/ab311c](https://doi.org/10.3847/1538-4357/ab311c)
- Papovich, C., Cole, J. W., Hu, W., et al. 2025, *arXiv e-prints*, arXiv:2505.08870, doi: [10.48550/arXiv.2505.08870](https://doi.org/10.48550/arXiv.2505.08870)
- Patton, D. R., Carlberg, R. G., Marzke, R. O., et al. 2000, *ApJ*, 536, 153, doi: [10.1086/308907](https://doi.org/10.1086/308907)
- Patton, D. R., Faria, L., Hani, M. H., et al. 2024, *MNRAS*, 529, 1493, doi: [10.1093/mnras/stae608](https://doi.org/10.1093/mnras/stae608)
- Patton, D. R., Torrey, P., Ellison, S. L., Mendel, J. T., & Scudder, J. M. 2013, *MNRAS*, 433, L59, doi: [10.1093/mnrasl/slt058](https://doi.org/10.1093/mnrasl/slt058)
- Pawlik, M. M., Wild, V., Walcher, C. J., et al. 2016, *MNRAS*, 456, 3032, doi: [10.1093/mnras/stv2878](https://doi.org/10.1093/mnras/stv2878)
- Pearson, S., Besla, G., Putman, M. E., et al. 2016, *MNRAS*, 459, 1827, doi: [10.1093/mnras/stw757](https://doi.org/10.1093/mnras/stw757)
- Pearson, W. J., Wang, L., Trayford, J. W., Petrillo, C. E., & van der Tak, F. F. S. 2019a, *A&A*, 626, A49, doi: [10.1051/0004-6361/201935355](https://doi.org/10.1051/0004-6361/201935355)
- Pearson, W. J., Wang, L., Alpaslan, M., et al. 2019b, *A&A*, 631, A51, doi: [10.1051/0004-6361/201936337](https://doi.org/10.1051/0004-6361/201936337)
- Purkayastha, S., Kanekar, N., Chengalur, J. N., et al. 2022, *ApJL*, 933, L11, doi: [10.3847/2041-8213/ac7522](https://doi.org/10.3847/2041-8213/ac7522)
- Purkayastha, S., Kanekar, N., Kumari, S., et al. 2024, *arXiv e-prints*, arXiv:2411.02527, doi: [10.48550/arXiv.2411.02527](https://doi.org/10.48550/arXiv.2411.02527)
- Ren, J., Liu, F. S., Li, N., et al. 2025, *arXiv e-prints*, arXiv:2507.23654, doi: [10.48550/arXiv.2507.23654](https://doi.org/10.48550/arXiv.2507.23654)
- Rey, M. P., Pontzen, A., Agertz, O., et al. 2022, *MNRAS*, 511, 5672, doi: [10.1093/mnras/stac502](https://doi.org/10.1093/mnras/stac502)
- Robaina, A. R., Bell, E. F., Skelton, R. E., et al. 2009, *ApJ*, 704, 324, doi: [10.1088/0004-637X/704/1/324](https://doi.org/10.1088/0004-637X/704/1/324)
- Robertson, B. E. 2022, *ARA&A*, 60, 121, doi: [10.1146/annurev-astro-120221-044656](https://doi.org/10.1146/annurev-astro-120221-044656)
- Rodriguez-Gomez, V., Snyder, G. F., Lotz, J. M., et al. 2019, *MNRAS*, 483, 4140, doi: [10.1093/mnras/sty3345](https://doi.org/10.1093/mnras/sty3345)
- Rosdahl, J., Blaizot, J., Katz, H., et al. 2022, *MNRAS*, 515, 2386, doi: [10.1093/mnras/stac1942](https://doi.org/10.1093/mnras/stac1942)
- Roy, N., Heckman, T., Henry, A., et al. 2024, *arXiv e-prints*, arXiv:2410.13254, <https://arxiv.org/abs/2410.13254>
- Saldana-Lopez, A., Schaerer, D., Chisholm, J., et al. 2022, *A&A*, 663, A59, doi: [10.1051/0004-6361/202141864](https://doi.org/10.1051/0004-6361/202141864)
- Saldana-Lopez, A., Hayes, M. J., Le Reste, A., et al. 2025, *arXiv e-prints*, arXiv:2504.07074, doi: [10.48550/arXiv.2504.07074](https://doi.org/10.48550/arXiv.2504.07074)
- Saxena, A., Pentericci, L., Ellis, R. S., et al. 2022, *MNRAS*, 511, 120, doi: [10.1093/mnras/stab3728](https://doi.org/10.1093/mnras/stab3728)
- Scarlata, C., Carollo, C. M., Lilly, S., et al. 2007, *ApJS*, 172, 406, doi: [10.1086/516582](https://doi.org/10.1086/516582)
- Scoville, N., Aussel, H., Brusa, M., et al. 2007, *ApJS*, 172, 1, doi: [10.1086/516585](https://doi.org/10.1086/516585)
- Smith, B. M., Windhorst, R. A., Teplitz, H., et al. 2024, *ApJ*, 964, 73, doi: [10.3847/1538-4357/ad1ef0](https://doi.org/10.3847/1538-4357/ad1ef0)
- Staveley-Smith, L., & Oosterloo, T. 2015, in *Advancing Astrophysics with the Square Kilometre Array (AASKA14)*, 167, doi: [10.22323/1.215.0167](https://doi.org/10.22323/1.215.0167)
- Steidel, C. C., Bogosavljević, M., Shapley, A. E., et al. 2018, *ApJ*, 869, 123, doi: [10.3847/1538-4357/aaed28](https://doi.org/10.3847/1538-4357/aaed28)
- Stierwalt, S., Besla, G., Patton, D., et al. 2015, *ApJ*, 805, 2, doi: [10.1088/0004-637X/805/1/2](https://doi.org/10.1088/0004-637X/805/1/2)
- Stinson, G. S., Dalcanton, J. J., Quinn, T., Kaufmann, T., & Wadsley, J. 2007, *ApJ*, 667, 170, doi: [10.1086/520504](https://doi.org/10.1086/520504)
- Toomre, A., & Toomre, J. 1972, *ApJ*, 178, 623, doi: [10.1086/151823](https://doi.org/10.1086/151823)
- Trebitsch, M., Blaizot, J., Rosdahl, J., Devriendt, J., & Slyz, A. 2017, *MNRAS*, 470, 224, doi: [10.1093/mnras/stx1060](https://doi.org/10.1093/mnras/stx1060)
- Trebitsch, M., Hutter, A., Dayal, P., et al. 2023, *MNRAS*, 518, 3576, doi: [10.1093/mnras/stac2138](https://doi.org/10.1093/mnras/stac2138)
- Trebitsch, M., Dayal, P., Chisholm, J., et al. 2022, *arXiv e-prints*, arXiv:2212.06177, doi: [10.48550/arXiv.2212.06177](https://doi.org/10.48550/arXiv.2212.06177)
- Vanzella, E., Nonino, M., Cupani, G., et al. 2018, *MNRAS*, 476, L15, doi: [10.1093/mnrasl/sly023](https://doi.org/10.1093/mnrasl/sly023)
- Veilleux, S., Kim, D. C., & Sanders, D. B. 2002, *ApJS*, 143, 315, doi: [10.1086/343844](https://doi.org/10.1086/343844)
- Ventou, E., Contini, T., Bouché, N., et al. 2019, *A&A*, 631, A87, doi: [10.1051/0004-6361/201935597](https://doi.org/10.1051/0004-6361/201935597)

- Virtanen, P., Gommers, R., Oliphant, T. E., et al. 2020, Nature Methods, 17, 261, doi: [10.1038/s41592-019-0686-2](https://doi.org/10.1038/s41592-019-0686-2)
- Walmsley, M., Smith, L., Lintott, C., et al. 2020, MNRAS, 491, 1554, doi: [10.1093/mnras/stz2816](https://doi.org/10.1093/mnras/stz2816)
- Wang, B., Heckman, T. M., Leitherer, C., et al. 2019, ApJ, 885, 57, doi: [10.3847/1538-4357/ab418f](https://doi.org/10.3847/1538-4357/ab418f)
- Wen, Z. Z., Zheng, X. Z., & An, F. X. 2014, ApJ, 787, 130, doi: [10.1088/0004-637X/787/2/130](https://doi.org/10.1088/0004-637X/787/2/130)
- Xu, X., Henry, A., Heckman, T., et al. 2022, ApJ, 933, 202, doi: [10.3847/1538-4357/ac7225](https://doi.org/10.3847/1538-4357/ac7225)
- Yeh, J. Y. C., Smith, A., Kannan, R., et al. 2023, MNRAS, 520, 2757, doi: [10.1093/mnras/stad210](https://doi.org/10.1093/mnras/stad210)
- Yuan, F.-T., Zheng, Z.-Y., Jiang, C., et al. 2024, ApJ, 975, 53, doi: [10.3847/1538-4357/ad75ff](https://doi.org/10.3847/1538-4357/ad75ff)
- Zhu, S., Zheng, Z.-y., Yuan, F.-T., Jiang, C., & Lin, R. 2024, arXiv e-prints, arXiv:2412.08395, doi: [10.48550/arXiv.2412.08395](https://doi.org/10.48550/arXiv.2412.08395)



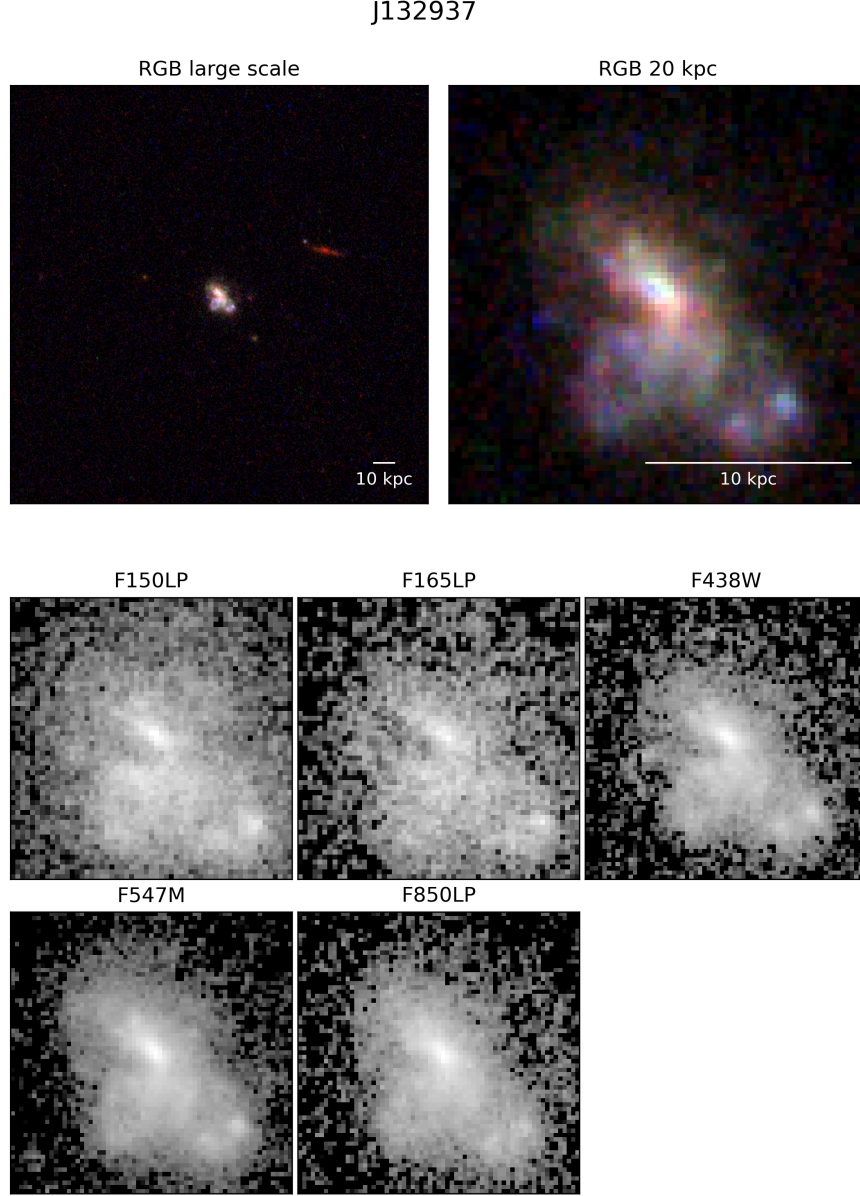


**Figure 9.** Example thumbnail shown to classifiers for merger identification.

## APPENDIX

### A. EXAMPLE IMAGE PANELS FOR CLASSIFICATION

On Figure 9 we show the example of an image panel presented to classifiers for the visual classification of galaxy J132937. This galaxy is classified as a robust galaxy merger near-coalescence with  $P_{\text{merg}} = 0.92$  and  $s_{\text{merg}} = 2.7$ . The two top panels show optical RGB images with scales chosen to maximize the visibility of structures across all filters. The top left panel shows a  $24''$ -wide image, the top right panels shows a 20kpc cutout of that image. The bottom panels show the same 20kpc cutouts for all available filters.

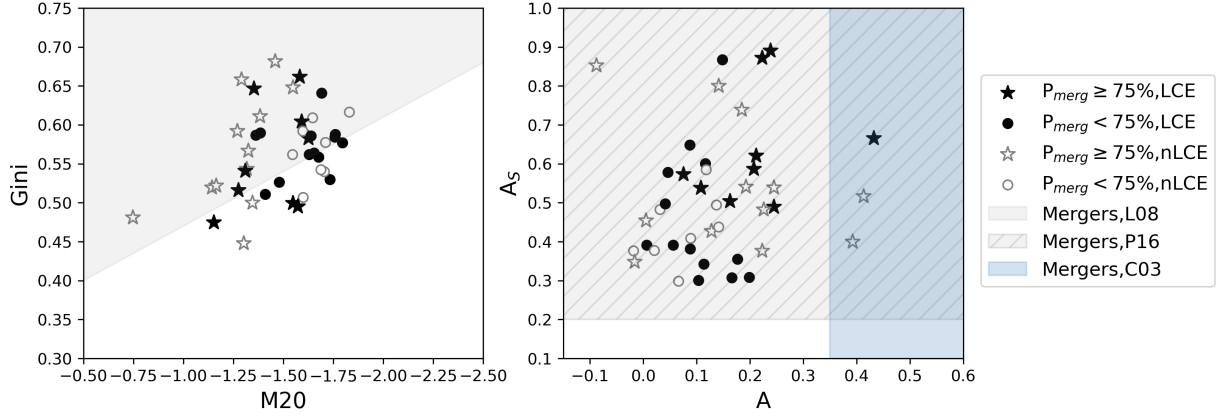


**Figure 10.** Visual merger classification as compared to morphometrics selection using F547M and F850LP images (closest to rest-frame B/g- and r/I-bands). The left panel shows the position of LaCOS galaxies on the Gini- $M_{20}$  diagram using F547M images, with the parameter space for merger in Lotz et al. (2008) overlaid in gray. The right panel shows LaCOS galaxies on the shape asymmetry and asymmetry diagrams using F850LP images, with the parameter space for merger in Conselice (2003) overlaid in blue and that in Pawlik et al. (2016) overlaid in gray.

## B. COMPARING VISUAL WITH NON-PARAMETRIC MORPHOLOGICAL MERGER IDENTIFICATION

Figure 10 presents the position of LaCOS galaxies on morphometric diagrams. Specifically, we show planes defined by merger selection criteria using the Gini and  $M_{20}$  coefficient ( $G > -0.14 * M_{20} + 0.33$  Lotz et al. 2008), the asymmetry ( $A \geq 0.35$  Conselice 2003) and the shape asymmetry ( $A_s \geq 0.2$  Pawlik et al. 2016). The latter parameter is more sensitive to faint isophotes than the traditional asymmetry, and has been developed to facilitate the identification of post-coalescence mergers. There is a large degree of variation in the galaxies identified or not as mergers via typical morphometrics criteria. While the asymmetry criterion selects only galaxies with high merger vote fraction, it fails to detect most of the robust mergers identified visually. The Gini- $M_{20}$  selection identifies about 75% of the robust mergers, but also selects 64% of the low vote fraction mergers. Finally, the selection based on shape asymmetry selects all of the LaCOS galaxies as mergers. These criteria were developed on B-band (Lotz et al. 2008), I-band (Conselice 2003) and r-band (Pawlik et al. 2016) images of relatively massive galaxies more representative of the general  $z \sim 0 - 1$  galaxy population, likely resulting in the low classification accuracy observed for LaCOS galaxies. This highlights the importance of considering the specifics of a given sample when selecting a merger classification scheme.